



HAL
open science

Mediterranean Mercury Assessment 2022: An Updated Budget, Health Consequences, and Research Perspectives

Daniel Cossa, Joël Knoery, Daniela Bănaru, Mireille Harmelin-Vivien, Jeroen Sonke, Ian Hedgecock, Andrea Bravo, Ginevra Rosati, Donata Canu, Milena Horvat, et al.

► **To cite this version:**

Daniel Cossa, Joël Knoery, Daniela Bănaru, Mireille Harmelin-Vivien, Jeroen Sonke, et al.. Mediterranean Mercury Assessment 2022: An Updated Budget, Health Consequences, and Research Perspectives. Environmental Science and Technology, 2022, pp.acs.est.1c03044. 10.1021/acs.est.1c03044 . hal-03600750

HAL Id: hal-03600750

<https://hal.science/hal-03600750v1>

Submitted on 15 Nov 2022

HAL is a multi-disciplinary open access archive for the deposit and dissemination of scientific research documents, whether they are published or not. The documents may come from teaching and research institutions in France or abroad, or from public or private research centers.

L'archive ouverte pluridisciplinaire **HAL**, est destinée au dépôt et à la diffusion de documents scientifiques de niveau recherche, publiés ou non, émanant des établissements d'enseignement et de recherche français ou étrangers, des laboratoires publics ou privés.

1 *Critical Review*

2 **Mediterranean Mercury Assessment 2022: An Updated** 3 **Budget, Health Consequences, and Research Perspectives**

4 *Daniel Cossa*^{1*}, *Joël Knoery*², *Daniela Bănar*³, *Mireille Harmelin-Vivien*³, *Jeroen E.*
5 *Sonke*⁴, *Ian M. Hedgecock*⁵, *Andrea G. Bravo*⁶, *Ginevra Rosati*⁷, *Donata Canu*⁷, *Milena*
6 *Horvat*⁸, *Francesca Sprovieri*⁵, *Nicola Pirrone*⁵, *Lars-Eric Heimbürger-Boavida*³

7 (1) *Université Grenoble Alpes, ISTERre, CS 40700, 38058 Grenoble Cedex 9, France;* (2)
8 *Ifremer, Centre Atlantique de Nantes, BP 44311, 44980 Nantes, France,* (3) *Aix Marseille*
9 *Université, CNRS/INSU, Université de Toulon, IRD, Mediterranean Institute of Oceanography*
10 *(MIO) UM 110, 13288 Marseille, France;* (4) *Géosciences Environnement Toulouse,*
11 *CNRS/Observatoire Midi-Pyrénées (OMP)/Université de Toulouse, 31400 Toulouse, France;*
12 (5) *Instituto sull'inquinamento atmosferico, CNR-IIA, 87036 Rende, Italy;* (6) *Institut de*
13 *Ciències del Mar, 08003 Barcelona, Spain;* (7) *Nazionale di Oceanografia e di Geofisica*
14 *Sperimentale (OGS), 34010 Trieste, Italy;* (8) *Institut Józef Stefan, 1000 Ljubljana, Slovenija.*

15 *Corresponding author, dcossa@ifremer.fr, ISTERre, Université Grenoble Alpes, CS 40700, 38058
16 Grenoble Cedex 9, France; Tel.: +1 438 939 6907.

17

18 **ABSTRACT:** Mercury (Hg) and especially its methylated species (MeHg) are toxic
19 chemicals that contaminate humans *via* the consumption of seafood. The most recent
20 UNEP Global Mercury Assessment stressed that Mediterranean populations have higher
21 Hg levels than people elsewhere in Europe. The present critical review updates current
22 knowledge on the sources, biogeochemical cycling, and mass balance of Hg in the
23 Mediterranean, and identifies perspectives for future research especially in the context of
24 global change. Concentrations of Hg in the Western Mediterranean average 0.86 ± 0.27
25 pmol L^{-1} in the upper water layer and $1.02 \pm 0.12 \text{ pmol L}^{-1}$ in intermediate and deep
26 waters. In the Eastern Mediterranean, Hg measurements are in the same range but are
27 too few to determine any consistent oceanographical pattern. The Mediterranean waters
28 have a high methylation capacity, with MeHg representing up to 86 % of the total Hg,
29 and constitute a source of MeHg for the adjacent North Atlantic Ocean. The highest
30 MeHg concentrations are associated with low oxygen water masses suggesting a
31 microbiological control on Hg methylation, consistent with the identification of *hgcA*-
32 like genes in Mediterranean waters. MeHg concentrations are twice as high in the waters
33 of the western basin compared to the ultra-oligotrophic eastern basin waters. This
34 difference appears to be transferred through the food webs and the Hg content in
35 predators to be ultimately controlled by MeHg concentrations of the waters of their
36 foraging zones. Many Mediterranean top-predatory fish still exceed European Union

37 regulatory Hg thresholds. This underlines the necessity of monitoring the exposure of
38 Mediterranean populations, to formulate adequate mitigation strategies and
39 recommendations, without advising against seafood consumption. This review also
40 points out other insufficiencies of knowledge of Hg cycling in the Mediterranean Sea,
41 including temporal variations in air-sea exchange, hydrothermal and cold seep inputs,
42 point sources, submarine groundwater discharge, and exchanges between margins and
43 the open sea. Future assessment of global change impacts under the Minamata
44 Convention Hg policy requires long-term observations and dedicated high-resolution
45 Earth System Models for the Mediterranean region.

46

47 **Introduction**

48 Mercury (Hg) has been classified by the United Nations Environment Programme
49 (UNEP) as a chemical element toxic to living organisms including humans^{1, 2, 3}. One
50 group of its compounds, methylated mercury (MeHg), damages the human nervous
51 system^{4, 5, 6}, and has been linked to cardiovascular disease⁷. Exposure of top predators to
52 MeHg is caused by its high biomagnification potential within aquatic food webs^{2, 8}.
53 Marine fish consumption is the main source of MeHg to humans^{2, 8, 9, 10}. Hg is of global
54 environmental concern, because of the major perturbation of its natural cycle by human
55 activities, its long-distance transport *via* the atmosphere resulting in its ubiquity in
56 terrestrial and marine ecosystems, and finally because of its long persistence in
57 biologically-crucial zones of the aquatic environment^{11, 12, 13}. The global issue of Hg has
58 begun to be confronted by the adoption of the Minamata Convention, which entered into
59 force in 2017 under the auspices of UNEP to reduce human and ecosystem Hg exposure.

60 The recent Global Mercury Assessment (GMA 2018)¹ highlighted key policy-
61 relevant findings and includes an updated inventory of anthropogenic Hg releases:
62 artisanal and small-scale gold mining, fossil fuel and biomass burning, waste
63 incineration, smelters, and from the re-mobilization of anthropogenic Hg deposited in
64 the past to soils, sediments, water bodies, dumping grounds, and mine-tailings.
65 Anthropogenic Hg emissions have been substantial since the Industrial Era, and have
66 left a detectable environmental imprint for more than 2000 years¹⁴. Moreover, it has
67 been estimated that 95 % of Hg emissions occurred in the last 500 years and that they
68 have increased by 1.8 % per year during the 2010-2015 period^{15, 16}. The global Hg
69 budget, updated in 2018¹³, states that current Hg concentrations in the global

70 atmosphere, surface, and deep marine waters have increased respectively by 450, 230,
71 and 12-25 % above levels prevailing during the pre-Colombian period¹¹, i.e., before
72 ~1450 CE. This budget however presents large uncertainties, in particular, local
73 differences are to be expected, due to specific geographical, geological, biological, and
74 anthropogenic factors.

75 The GMA 2018¹ also stresses that Mediterranean (MED) populations tend to have
76 higher Hg levels than people from Asia, North America, and Europe. Already, 50 years
77 ago, high Hg levels were observed in MED fish and marine mammals^{17, 18}, and these
78 findings have been confirmed several times^{19, 20, 21}. It has been recently suggested that
79 Hg accumulation rates in bluefin tuna are the highest in the individuals from the MED²²
80 and that certain birds linked to the marine ecosystem could be at risk of suffering long-
81 term, Hg-related effects²³. These observations suggest specific features and a particular
82 vulnerability of this region and emphasize the need to reassess, there, the state of the art
83 on Hg. The present Critical Review aims to summarize and update current knowledge on
84 the biogeochemistry of Hg in the MED, including its main implications for human
85 health, and to identify perspectives for future research activities in this field.

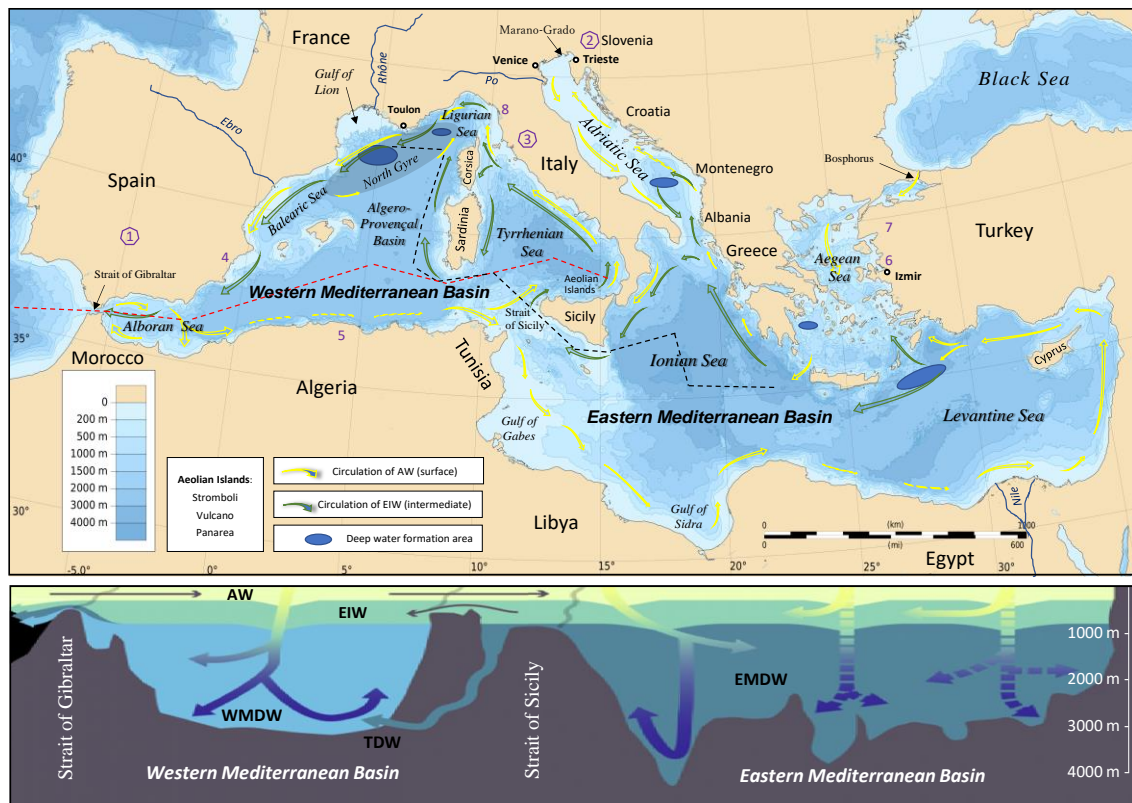
86

87 **1. The marine mercury cycle and relevant Mediterranean-specific features**

88 The main chemical reactions within the Hg cycle in the environment may be roughly
89 summarized by the interconversions of elemental Hg (Hg^0), inorganic divalent Hg (Hg_i^{II}),
90 and organic divalent, including mono- and dimethylated species (CH_3Hg^+ /MMHg and
91 CH_3HgCH_3 /DMHg, hereafter collectively abbreviated as MeHg). Mobility through the
92 atmosphere is favored by volatile Hg^0 , and through the hydrosphere by the solubilities of
93 various Hg^{II} species. A summary of the latest scientific advances on the global Hg
94 biogeochemical cycle is available in a recent paper²⁴. Due to its volatility, Hg is dispersed
95 in the global atmosphere. Part of it is redeposited onto continental and sea surfaces, where
96 it is incorporated into biota mainly as MeHg. MeHg biomagnification along the food web
97 is its main source of Hg for top predators, with a bioconcentration factor up to 10^7 (Ref.
98 25). The result is that some marine predators eaten by human populations or other
99 animals are the main sources of their exposure to MeHg and as such a major risk of Hg
100 poisoning⁸. A more detailed summary of the biogeochemical Hg cycle is given in the
101 Supporting Information (SI.1).

102 The MED is a semi-enclosed sea (Fig. 1), with a water residence time of around 100
 103 years, characterized by marked North-South and East-West gradients, mainly driven by
 104 the different physiographies of the two basins, the different terrestrial nutrient loadings,
 105 and the cyclonic and anticyclonic wind-driven current structures^{26, 27}. The geological
 106 context, the contrasting hydrodynamic regimes, and the biogeochemical functioning of
 107 the MED have several characteristics important to the MED Hg cycle. In addition, the
 108 MED has been identified as a climate change hotspot^{28, 29}.

109



110

111 **Figure 1.** The Mediterranean Sea with its main rivers and a schematic of water circulation.
 112 Purple numbers refer to Hg ore deposits: (1) Almaden, Spain, (2) Idrija, Slovenia, and (3) Monte
 113 Amiata are the main ones; other minor Hg deposits include (4) Azogue Valley (Pulpi), Spain, (5)
 114 Numidia, Algeria, (6) Karaburn, Turkey, (7) Kuçukyeniçe, Turkey, and (8) Levigliani, Italy. The
 115 red dash line refers to the Figure 2 transect. The black dash line refers to the Figure 3 transect.
 116 Dash arrows refer to seasonal circulation paths. The lower part of the figure is modified from
 117 Ref. 27. www.ifremer.fr/lobtln/COURANTS/SCHEMA_3D_MED_LABELS_EN.jpg.

118 The Iberian Hg belt, where cinnabar (HgS) is the principal Hg ore, is found along
 119 the edges of the MED. It extends from Spain (Almaden) to Italy (Monte Amiata),
 120 Slovenia (Idrija), Algeria (Numidia belt), and Aegean Turkey (Karaburun) (Fig. 1). In
 121 addition to these natural sources, mining and other anthropogenic activities have
 122 mobilized large quantities of Hg that are now buried in coastal sediments. Among the

123 most relevant anthropogenic legacy Hg hotspots in the MED, are the Gulf of Trieste
124 (with 13 000 Mg of anthropogenic Hg accumulated in the sediments^{30, 31}), Marano
125 Grado Lagoon (271 Mg³²), Venice Lagoon (20 Mg³³) in the Eastern MED (EMED), and
126 the Toulon Bay (26 Mg³⁴) in the Western MED (WMED) (Fig. 1). These Hg reservoirs
127 can maintain steady inputs to the water column. Also, Hg-laden sediments may be
128 remobilized and transported off-shore during floods or storms. Mercury inputs to the
129 MED from hydrothermal vents are suspected but are not yet constrained³⁵. Elevated Hg
130 concentrations have been found in shallow hydrothermal fluids³⁶ and terrestrial
131 volcanoes³⁷. Subaerial volcanic Hg emissions in the Mediterranean region are dominated
132 by the Aeolian Island volcanoes Vulcano and Stromboli, and by Mt Etna in Sicily³⁸ (Fig.
133 1).

134 Since it has become possible to determine accurately ultra-trace levels of Hg in
135 ocean waters, several mass budgets for Hg in the MED have been established^{39, 40, 41}.
136 The first budget concludes that Hg entered through the Gibraltar Strait as inorganic Hg
137 and was exported to the North Atlantic Ocean with a larger proportion of MeHg³⁹.
138 Another conclusion was that atmospheric exchanges are the main source and sink of Hg
139 in the MED⁴¹. Hg exchanges at the sediment/water interface and the influence of
140 hydrothermal vents are currently much less well constrained. The ultimate sources of
141 water-column MeHg are currently under debate^{42, 43}. The experimental estimates of Hg
142 methylation rates^{44, 45} suggest that the consequence of even a small change in these
143 transformation rates would have a major impact on the levels of MeHg, which is the
144 main factor governing the entry of Hg into the food webs. Continental Hg sources,
145 namely rivers and groundwaters, have not yet been considered with sufficient attention
146 in the karstic MED environment. Large discrepancies also exist between estimates of Hg
147 transport in water masses, due to variations in Hg water column concentrations over the
148 last 30 years^{39, 40, 41}. These variations in Hg flux estimates may be due to (i) the observed
149 decrease in Hg concentrations in North-Atlantic surface waters which can be over 50 %
150 between 1989 and 2012⁴⁶, but also to (ii) variations in the surface water inflow estimated
151 at Gibraltar⁴⁷. Furthermore, the residence time of water in the WMED is shorter than 50
152 years and biogeochemical conditions and Hg fluxes may vary over a decadal time
153 scale^{27, 29}. In summary, the steady-state Hg fluxes in the different MED biogeochemical
154 compartments are far from being well-established, warranting a revisit of Mediterranean
155 Hg dynamics and budget. Moreover, Hg accumulation in biota is a multi-causal

156 process^{21, 48} that is ultimately determined not only by past Hg emissions and their
157 temporal evolution, but also by changes in biogeochemical, climate-induced, and
158 biologically mediated processes⁴⁹. Thus, the ecological and health consequences of the
159 present Hg cycle in the MED will likely further evolve with the climate changes
160 expected over the next decades.

161

162 **2. Updating the Mediterranean Hg cycle**

163 **2.1. Emissions, evasions, and deposition**

164 An early assessment of the total anthropogenic Hg emissions of countries bordering the
165 MED was about 100 Mg for the year 1995 (i.e., equivalent to a third of European or 5%
166 of global anthropogenic emissions)⁵⁰. Thirty (30) Mg resulted from the burning of fossil
167 fuels, 29 Mg from the incineration of household wastes, 28 Mg from cement production,
168 and 10 Mg from the production of chlorine and lye. In addition, the total amount of Hg
169 released to the atmosphere from forest fires in the Mediterranean region accounted for
170 4.3 Mg y⁻¹ (Ref. 51) and 7 Mg y⁻¹ from volcanoes (see section 2.5.). The GMA 2018¹
171 indicates that between 2010 and 2015 anthropogenic emissions from the (then) EU28
172 (EU28 was the abbreviation of the 28 countries of the European Union) decreased by
173 12.5 % while those from North Africa increased slightly (+15.8 %). Both EU28 and
174 North Africa increased in large-scale gold production, and while the EU28 countries
175 reduced emissions from the oil industry and power plants, North Africa increased
176 emissions from domestic and industrial fossil fuel combustions. The phasing out of Hg
177 in chlor-alkali plants in EU28 led to a two-thirds reduction in emissions from chemical
178 industries.

179 Since the year 2000, numerous oceanographic and more local near-coast
180 measurement campaigns have been carried out to determine Hg species concentrations
181 in the marine boundary layer and the water column^{52, 53, 54, 55, 56}. Evasion fluxes of Hg are
182 calculated using measured dissolved gaseous mercury (DGM) and Hg^{0(g)} concentrations,
183 wind speed, and sea surface temperature, and several approaches can and have been
184 used to estimate MED efflux/volatilization/atmospheric rates^{57, 58, 59, 60}. Details about the
185 medalling approaches to calculate gas transfer velocities at the air-sea interface are given
186 in Supporting Information (SI.2)^{61, 62, 63, 64, 65, 66, 67, 68, 69, 70, 71}.

187 Averaged Hg evasion fluxes for the MED are reasonably consistent across the
188 literature, 2-8 ng m⁻² h⁻¹, with higher values typically found in summer and autumn (up
189 to 20 ng m⁻² h⁻¹ was reported⁶⁰ for a short period), and for the Eastern Basin compared to
190 the Western Basin^{57, 58, 59, 60}. The higher values obtained for the Eastern Basin stem
191 possibly from tectonic activity. These fluxes lead to estimates of annual evasion of Hg⁰
192 to the atmosphere between 50 and 100 Mg y⁻¹ (Table 4 in Ref. 71). While the estimated
193 average fluxes are close between the studies, all the above studies indicate that the Hg⁰
194 flux to the atmosphere can be extremely variable over space and time. Indeed, they
195 depend on DGM concentrations, temperature, and exponentially on wind speed, which
196 are all highly variable. There are also several Hg “hot spots” in the MED, both due to
197 tectonic activity and regions impacted by anthropogenic activities where significantly
198 higher evasion fluxes can occur^{72, 73}. A description of atmosphere surface exchange
199 measurement techniques can be found in a recent review⁷⁴.

200 Mercury deposition to the MED is a combination of Hg^{II} wet deposition (rainfall),
201 dry deposition of gaseous, and particulate oxidized Hg^{II} forms. There are several
202 “European Monitoring and Evaluation Programme” sites that measure Hg wet and/or
203 dry depositions. Unfortunately, only 3 of these are in or near the MED basin, and
204 measure wet deposition only: Iskrba, Slovenia, at 500 m a.s.l., Longobucco, in Southern
205 Italy, at 1358 m a.s.l., and Ostriconi, in Corsica, at 100 m a.s.l. Annual Hg wet
206 deposition at these sites is 6.7, 1.7, and 3.0 µg m⁻² y⁻¹ respectively^{75, 76}. The paucity of
207 representative measurement data for the MED is an issue that needs to be addressed. Hg
208 deposition to the MED has therefore been estimated from knowledge of the
209 concentration of Hg⁰ and its oxidants in the region, the rate of atmospheric oxidation
210 processes which lead to the formation of Hg^{II}, and wet and dry deposition processes.
211 Gencarelli et al.⁷⁷ used a version of WRF-Chem to estimate dry and wet deposition
212 fluxes to the MED. They found that the modeled contributions to deposition were almost
213 equal, 19.6 and 18.1 Mg y⁻¹ dry and wet, respectively. No observational data exist for
214 Hg dry deposition. Combined with modeled annual evasion of Hg⁰ from the sea surface
215 of 67.5 Mg y⁻¹ (in agreement with most of the estimates from the studies above), the
216 model budget gives a net annual evasion flux of 30 Mg. A further model study showed
217 that dry deposition accounted for more than half the Hg deposited to the MED in the
218 summer months, and between 40 and 50 % of the annual total deposition, depending on
219 the atmospheric Hg oxidation mechanism employed in the model⁷⁸. Synoptic scale wet

220 deposition of Hg contributes roughly ten times more to the total Hg deposition than
221 convective wet deposition and is the dominant source of Hg to the MED from Autumn
222 through to Spring. Most Hg deposition to the MED is due to transport from distant
223 sources, except in the summer when sources from countries surrounding the MED have
224 a greater influence due to the prevailing meteorological conditions. This is reflected in
225 the change in the total modeled deposition to the MED when using anthropogenic
226 emission databases for 2005 and 2010, where a 33 % reduction of in-domain emissions
227 resulted in a 12 % deposition decrease. A global modeling study⁷⁹ suggested that slightly
228 more than 20 % of Hg deposited to the MED comes from primary anthropogenic
229 sources. A recent study⁸⁰ estimates that a 50 % reduction in EU emissions, would only
230 lead to a 17 % decrease in Hg deposition to the MED.

231 The recent advances in understanding the processes driving atmospheric Hg redox
232 chemistry^{81, 82, 83, 84}, and also in coupling ocean and atmosphere models^{69, 71}, suggest that
233 it would be an appropriate time for high-resolution MED modeling studies to be
234 conducted again. Potentially the photolytic reduction of Hg^{II} compounds in the
235 atmosphere⁸² could have a significant role in the cycling of Hg between the atmosphere
236 and seas. Gas-phase reduction of Hg^{II} could decrease model estimates of both Hg^{II} wet
237 and dry deposition to the MED, by a proportion that needs yet to be modeled. Given the
238 dominance of Hg long-range transport and the synoptic rain fluxes, the chemical
239 reduction of gaseous Hg^{II} likely has a small impact. Gas-phase reduction of Hg^{II} could
240 decrease model estimates of both Hg^{II} wet and dry deposition to the MED, by a
241 proportion that needs yet to be modeled, and that is supported by recent Hg stable
242 isotope observations of Hg in the MED⁸⁵.

243 Despite the questions remaining regarding the exact nature of atmospheric Hg redox
244 pathways, there is little doubt that the MED is a net source of Hg to the atmosphere,
245 with roughly 60 - 80 Mg y⁻¹ is emitted to the atmosphere while it is estimated that dry
246 and wet deposition amount at around 20 Mg y⁻¹ each.

247 ***2.2. The waters of the Mediterranean Sea***

248 *2.2.1. Geographical distribution of total mercury (THg)*

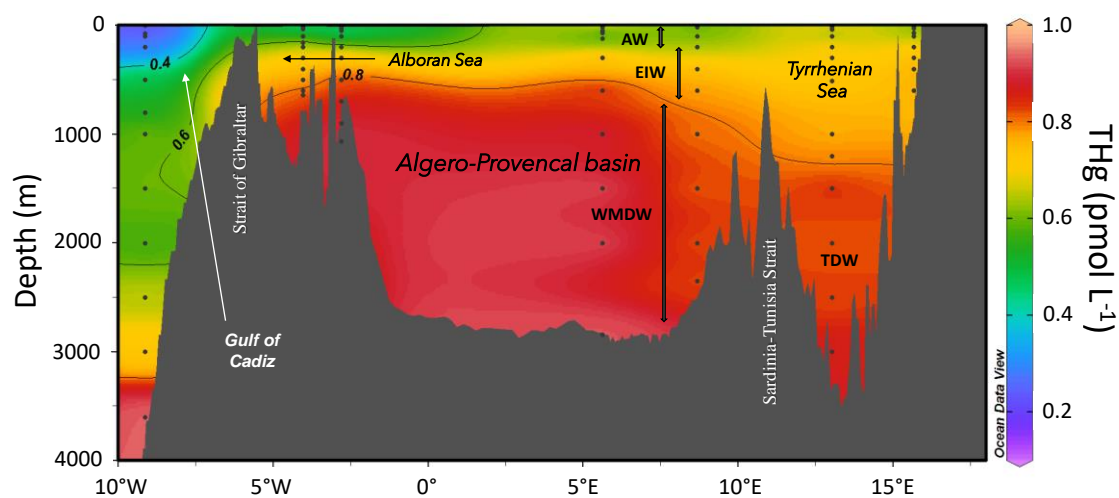
249 The vertical structure of the WMED water column can be schematically subdivided into
250 three major water masses: (i) Atlantic Water (AW), (ii) Eastern Intermediate Water
251 (EIW), and (iii) Western Mediterranean Deep Water (WMDW)²⁷ (Fig. 1). AW (from the

252 surface to ~ 250 m) is a low salinity water mass entering the MED at Gibraltar, and
253 spreading eastward into the entire basin. EIW is a high salinity water mass, located just
254 below AW and down to ~600 m, originating in the EMED. Below that depth and down
255 to the seabed is the WMDW formed in the WMED during winter convection periods,
256 which fills the entire basin. In addition, in the Tyrrhenian basin, Tyrrhenian Deep Water
257 (TDW) is formed as the result of the deep mixing of waters from eastern and western
258 MED (Fig. 1).

259 Figure 2 illustrates a recently measured distribution of THg across the western basin
260 (WMED). Summarized statistics of THg concentrations (pmol L^{-1}) in the WMED waters
261 measured between 2000 and 2017 are given in the Supporting Information (SI.3). In
262 open waters, the $<0.45 \mu\text{m}$ fraction represents 89% of the THg in waters. High and low
263 THg concentrations are present in the AW ($0.21\text{-}2.01 \text{ pmol L}^{-1}$) averaging 0.86 ± 0.27
264 pmol L^{-1} . Within the EIW and WMDW, the concentrations vary over a narrower range
265 ($0.51\text{-}1.62 \text{ pmol L}^{-1}$) averaging $1.02 \pm 0.12 \text{ pmol L}^{-1}$. The highly variable concentrations
266 in AW are the consequence of air-sea exchange dynamics which govern the balance
267 between Hg deposition and evasion from the sea surface, and primary production, which
268 governs the downward Hg biological pump. In places where deep convection occurs
269 (i.e., the Ligurian Sea and the Gulf of Lion), transferring the surface layer and its Hg
270 level to depth, a local Hg-enrichment (or depletion) of the WMDW can be observed
271 compared to the rest of the Western Basin. By comparison, the THg concentrations in
272 the waters of the WMED margins (Gulf of Lion) are slightly higher: $1.52 \pm 1.00 \text{ pmol L}^{-1}$
273 1 in the inner shelf, $1.09 \pm 0.15 \text{ pmol L}^{-1}$ along the slope, and $1.10 \pm 0.13 \text{ pmol L}^{-1}$ in the
274 Northern Gyre. These higher concentrations result from the higher particulate Hg load of
275 shelf waters⁸⁶ rather than dissolved Hg species. In the open waters of the eastern basin
276 (EMED) Hg measurements are scarce. The first “oceanographically consistent” profile
277 showed little vertical THg variation (mean = $1.01 \pm 0.08 \text{ pmol L}^{-1}$, $n = 22$)⁷⁵. Note that
278 “oceanographic consistency” means, among other criteria, that vertical profiles should
279 be smooth and relatable to established oceanographic features⁸⁷. In contrast, more data
280 are available from the Adriatic Sea. This region, consisting of a large continental shelf,
281 exhibits high THg concentrations and strong geographical gradients due to Hg mining
282 and industrial sources⁸⁸.

283 No temporal trend has been detected in the THg concentrations listed in the
284 Supporting Information (SI.3). However, a significant decrease in concentration in the

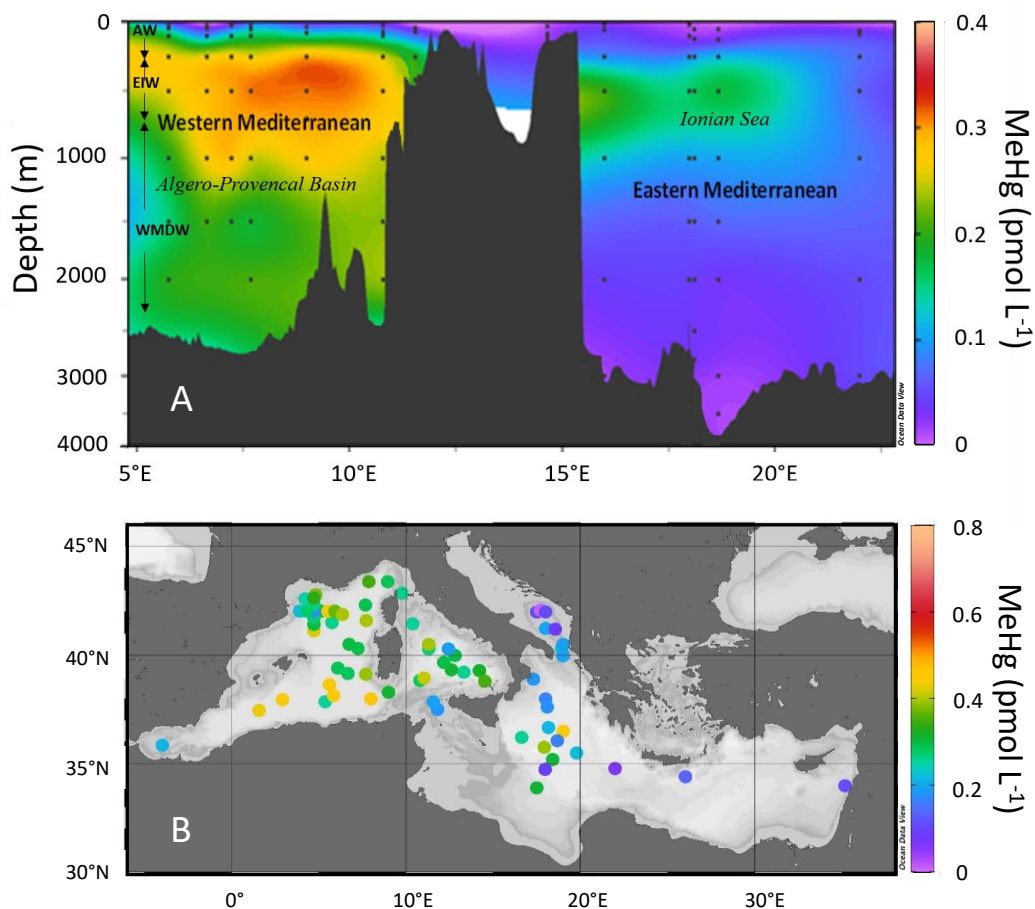
285 Alboran Sea and the adjacent Northeast Atlantic waters was observed over a 20-year
286 period⁴⁶. Based on the results of THg in water columns on both sides of the Strait of
287 Gibraltar between 1989 and 2012, it was proposed that a 30 % decrease of THg has
288 occurred in the deep layer which flows out of the MED, whereas a 50 % decrease has
289 occurred in the Atlantic waters entering the MED.



290

291 **Figure 2.** Distribution of total Hg in unfiltered samples (THg) distribution across the WMED
292 during FENICE cruise (2012). AW: Atlantic Water, EIW: Eastern Intermediate Water, WMDW:
293 Western Mediterranean Deep Water, TDW: Tyrrhenian Deep Water. The path of the transect is
294 the red dash line in Figure 1.

295



297

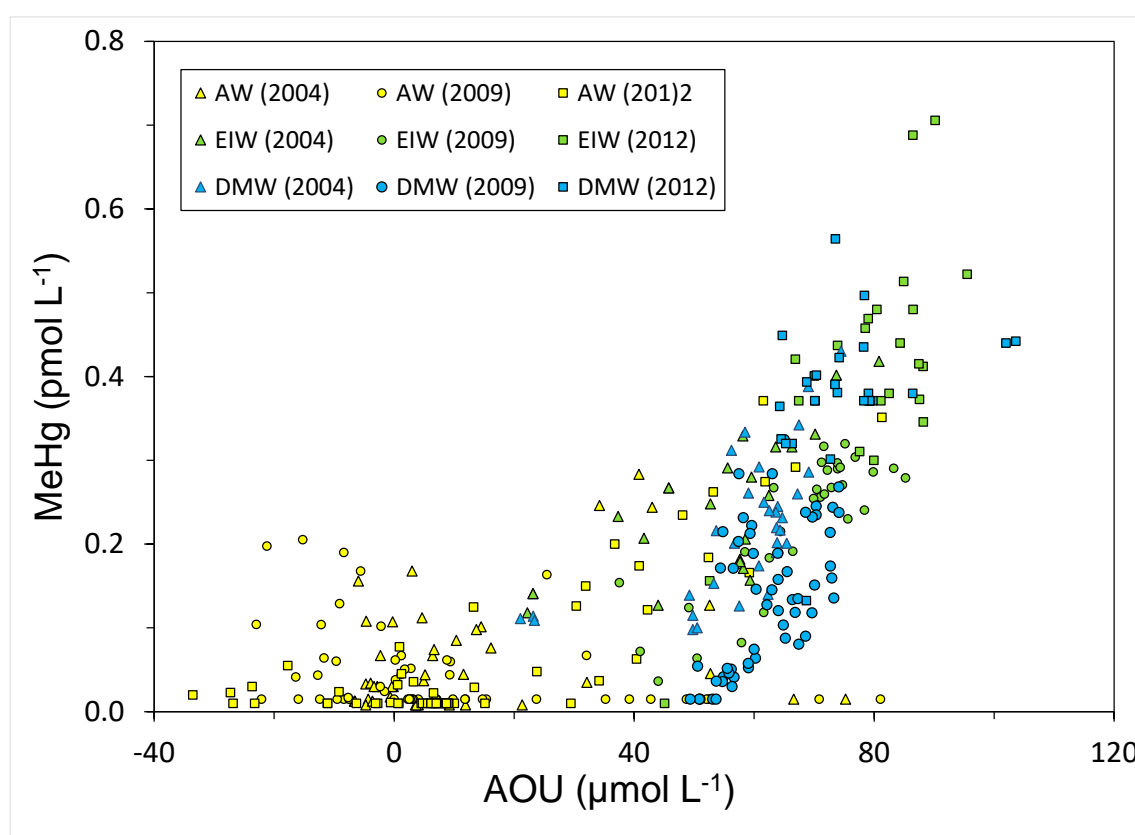
298 **Figure 3.** Panel A: Methylated Hg (MeHg) in unfiltered samples during ALDEBARAN cruise
 299 (June 2009). AW: Atlantic Water, EIW: Eastern Intermediate Water, WMDW: Western
 300 Mediterranean Deep Water, TDW: Tyrrhenian Deep Water. The path of the transect is the black
 301 dash line in Figure 1. Panel B: MeHg in unfiltered samples from 400 m during MEDSHIP cruise
 302 (2011).

303

304 Recent MeHg measurements^{89, 90} display concentration ranges from $<0.02 \text{ pmol L}^{-1}$
 305 up to 0.71 and up to 0.23 pmol L^{-1} for the WMED and EMED waters, respectively. The
 306 MeHg:THg ratios vary from 0.01 to 0.86. The highest values are found in the oxygen
 307 minimum zones (OMZ). These ranges are similar to other ocean basins (Supporting
 308 Information, SI.4). MeHg concentrations vary spatially (Fig. 3) with higher levels in the
 309 WMED compared to the EMED, and over-time as shown by time-series in the Ligurian
 310 Sea (WMED)⁹¹. MeHg was positively correlated with oxygen consumption (Fig. 4),
 311 especially within aphotic layers, namely EIW and DMW ($\text{MeHg}_{\text{pM}} = 0.004 \text{ AOU}_{\mu\text{M}} -$
 312 0.017 ($R^2 = 0.58$, $n = 301$, $p < 0.001$). Regression coefficients (molar ratios) of MeHg vs

313 apparent oxygen utilization (AOU) relationships, assumed to be a proxy for the Hg
 314 methylation capacity of a water mass, varied between 2.1×10^{-3} and 6.6×10^{-3} during a
 315 number of Mediterranean cruises. Compared with values obtained in the North,
 316 Equatorial, South Pacific^{92, 93}, the Southern Ocean⁹⁴, and the North Atlantic⁹⁵, the
 317 methylation capacity of intermediate waters of the MED is the highest. Methylation in
 318 the OMZ results from microbiological activity in association with OM regeneration^{92, 96,}
 319 ^{97, 98}. Low MeHg concentrations were found in waters overlying the continental shelves
 320 of the Northern Adriatic and Gulf of Lion^{43, 88}.

321



322

323 **Figure 4.** Methylated Hg (MeHg) vs. Apparent Oxygen Utilization (AOU) during MEDOCEANOR-
 324 3 (April 2004), ALDEBARAN (June 2009), and FENICE cruises (August 2012). Colors refer to
 325 various water masses (yellow for AW, green for EIW, and blue for DMW, Fig. 1). The shapes of
 326 symbols refer to the different cruises.

327 Mono- and dimethylmercury have been identified in Mediterranean waters^{39, 43, 99}.
 328 However, observed MMHg:DMHg ratios vary inexplicably in space and time. This
 329 possibly indicates a very fast interconversion of the two Hg methylated species or more
 330 likely analytical difficulties. Thus, the first step to address this issue would be to acquire
 331 additional quality-controlled data on Hg speciation. The second step would be to further

332 explore the mechanisms for Hg_i^{II} methylation in oxic oceanic waters. Suboxic/anoxic
333 microzones of the marine snow may be suitable environments for microbiological Hg
334 methylation, as has been suggested for settling particles in lakes¹⁰⁰. In marine
335 oligotrophic waters, such as those of the EMED, findings suggest an important role for a
336 noncellular or extracellular methylation mechanism¹⁰¹.

337 *2.2.3. Dissolved gaseous Hg*

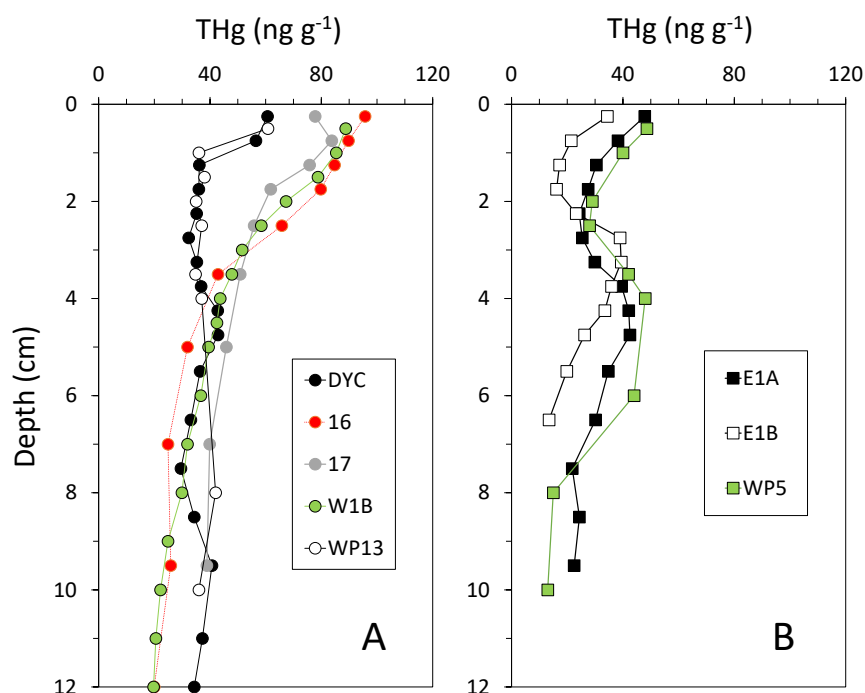
338 Generally, DGM represents 1/5th of the THg in Mediterranean waters and it would
339 consist, mostly of dissolved Hg^0 if DMHg data are correct. Vertical profiles of DGM
340 presents large spatial and temporal variations from a few tenths to 1.4 pmol L⁻¹, with
341 high concentrations found in intermediate and deep waters (e.g., EIW, WMDW, and
342 EMDW) compared to AW⁸⁸, and frequent increases in the hypoxic layer. This is
343 coherent with a microbially-mediated Hg reduction to DGM species. Finally, a possible
344 geotectonic origin for DGM exists in the hydrothermal zones of the MED¹⁰². In coastal
345 areas of the Adriatic Sea, the influence of anthropogenic Hg on DGM has been
346 suggested⁸⁸.

347 *2.3. The sediments of the Mediterranean Sea*

348 Sediment cores were collected on the abyssal plain of the MED^{42, 75, 103}. Some THg
349 vertical profiles in sediment cores from the abyssal plain of the MED are shown in
350 Figure 5. The use of Hg stable isotopes allowed us to suggest anthropogenic sources for
351 Hg in Mediterranean surface sediments¹⁰⁴. A recent paper¹⁰⁵ shows that Hg
352 accumulation rates rose from 0.4 to 8.6 $\mu\text{g m}^{-2} \text{y}^{-1}$ in the last 6000 years, with a
353 maximum deposition in the last 120 years. According to the same authors, the
354 accumulation rate for the year 2001-2002 measured with a sediment trap, located 20 m
355 above abyssal sediments, was $3.1 \pm 0.5 \mu\text{g m}^{-2} \text{y}^{-1}$ and suggests to Hg fluxes to the deep
356 WMED sediments of 4.2 Mg y^{-1} . The rare MeHg determinations in open MED
357 sediments indicate that it would represent between 0.5 to 2 % of the THg^{42, 106}. A MeHg
358 diffusive flux from deep sediments to the water column was estimated between 0.2 and
359 $2.3 \mu\text{g m}^{-2} \text{y}^{-1}$ (Ref. 42), which represents more than 50% of the deposition; these are
360 probably largely overrated. For the EMED deep sediments, we based our calculation on
361 a sedimentation rate ratio of 0.68 between EMED and WMED¹⁰⁷ and a Hg concentration
362 in EMED surface sediment of half of the WMED (Fig. 5). With these assumptions, the
363 Hg accumulated each year in the deep sediment of the EMED is ca. 1.6 Mg. Mercury
364 accumulation on MED coastal sediments is more documented particularly on the shelves

365 of the Gulf of Lion (WMED)⁸⁶ and of the Adriatic Sea (EMED)^{88, 108} where Hg hotspots
 366 were identified. Extrapolating these data, the Hg accumulated each year on the shelf is
 367 3.6 and 3.2 Mg for Western and Eastern basin shelf sediments, respectively. However,
 368 the shelf sediments may not be a permanent sink, and turbiditic currents and cascading
 369 phenomena may export part of the sediment to the abyssal plain trough canyons¹⁰⁹.

370



371

372 **Figure 5.** Total Hg concentration (THg) profiles in sediment cores from the abyssal plain
 373 (bottom > 2000m) of the Western Mediterranean (A) and Eastern Mediterranean (B). (DYC)
 374 Ligurian Sea¹⁰³; (WP13, WIB, 16 and 17) Algero-Provençal basin^{42, 75}; (EIA and E1B) Ionian
 375 Sea⁷⁵; (WP5) Levantine Sea⁴².

376 2.4. Exchanges with the Atlantic Ocean

377 Using water mass fluxes and updated THg concentrations from Table 1, the Hg inflow
 378 entering the MED at the Strait of Gibraltar is $2.54 \pm 0.26 \text{ Mg y}^{-1}$. This estimation is more
 379 than 3 times lower than the 7.5 Mg y^{-1} estimated in the previous budget⁴¹. On the other
 380 hand, Hg outflow to the North Atlantic Ocean is $3.99 \pm 0.76 \text{ Mg y}^{-1}$, a value also smaller
 381 than the preceding estimate (6.5 Mg y^{-1})⁴¹. The largest difference of this budget
 382 compared to the previous transport calculation at the Gibraltar Strait is the net export of
 383 “Mediterranean Hg” to the adjacent North Atlantic Ocean of $\sim 1.9 \text{ Mg y}^{-1}$. This export is
 384 consistent with the Hg-enriched Mediterranean water lenses found at the salinity
 385 maximum in the North-East Atlantic Ocean water column¹¹⁰. Thus, the MED is a source

386 of Hg for the adjacent Eastern North Atlantic Ocean, as it is also for lead¹¹¹, another
 387 anthropogenic trace metal still abundant in the MED. Considering the MeHg fluxes, the
 388 excess of Mediterranean export to the Atlantic is more marked, since MeHg is maximum
 389 at depth (with outflowing waters at Strait of Gibraltar) and demethylation of MeHg
 390 occurs in inflowing surface waters. Using the water fluxes at Gibraltar of 0.85 Sv and
 391 the MeHg concentrations of 0.25 pmol L⁻¹, this export of Mediterranean MeHg to the
 392 North Atlantic Ocean is 1.35 Mg y⁻¹.

393 **Table 1.** Average concentrations (\pm standard deviation) of total Hg (THg) and methylated Hg
 394 (MeHg) and derived fluxes at the Strait of Gibraltar. 1 Sv = 10⁶ m³ s⁻¹. (*) at Espartel sill
 395 according to Ref. 112. THg concentrations from Ref. 46. MeHg concentrations from Ref. 90.

Water mass	Water flux* (Sv)	THg (pmol L ⁻¹)	Hg flux (kmol y ⁻¹)	MeHg (pmol L ⁻¹)	MeHg flux (kmol y ⁻¹)
Atlantic inflow	0.89 \pm 0.12	0.45 \pm 0.05	12.6 \pm 2.3	<0.05	<1.4
Mediterranean outflow	0.85 \pm 0.13	0.83 \pm 0.13	22.3 \pm 3.8	0.26 \pm 0.09	6.9 \pm 1.2

396 2.5. Volcanic and hydrothermal emissions

397 Subaerial volcanic Hg emissions in the Mediterranean region are dominated by the
 398 Aeolian volcanoes Vulcano and Stromboli, and by Mt Etna in Sicily. A cruise campaign
 399 to the south-western sector of the Mediterranean Basin during summer 2015 studied the
 400 potential impact of continuously active volcanoes of the Aeolian arc on observed
 401 atmospheric Hg concentrations¹¹³. Increases in GOM (Gaseous Oxidized Mercury)
 402 concentrations, often during night time (30 pg m⁻³ with peaks of 129 pg m⁻³), were
 403 observed close to Stromboli volcano in the air originating from it, simultaneously with
 404 an increase in both SO₂ and GEM (Gaseous Elemental Mercury). There are currently
 405 many difficulties in quantifying the Hg flux from volcanic emissions due to the spatial
 406 and temporal variabilities in the activity from one volcano to another^{37, 114}, or from
 407 different emission sites on the volcano¹¹⁵.

408 Ferrara et al.³⁷ measured Hg/SO₂ ratios at Vulcano and used these to calculate
 409 passive Hg emissions ranges for Vulcano (1.3 – 5.5 kg y⁻¹), Stromboli (7.3 – 77 kg y⁻¹),
 410 and Etna (0.06 – 0.54 Mg y⁻¹) by multiplying with field-based SO₂ emission estimates.
 411 Here we use a mean global volcanic Hg/SO₂ ratio of 7.8 \pm 1.5 \times 10⁻⁶ (n = 13, Ref. 116)
 412 and modern satellite-based SO₂ emissions for Stromboli and Etna¹¹⁷ between 2005-2015
 413 to estimate passive degassing Hg emissions of 0.5 \pm 0.3 Mg y⁻¹ for Stromboli and 5.8 \pm

414 1.8 Mg y⁻¹ for Etna. Remote sensing SO₂ data is not available for Vulcano, so we cannot
415 refine its budget here. Global eruptive volcanic SO₂ emissions, estimated by remote
416 sensing, are indicated to be one order of magnitude smaller (8.8x) than passive
417 degassing¹¹⁷. We, therefore, estimate the sum of passive and eruptive aerial volcanic Hg
418 emissions in the MED region to be 7.0 ± 2.3 Mg y⁻¹.

419 Two recent GEOTRACES cruises found elevated Hg levels crossing the Mid Atlantic
420 Ridge and no distinct Hg signal crossing the East Pacific Rise in the vent plumes^{118, 119}.
421 The results and implications are either contradictory or point to strong site-specificity
422 and temporal dynamics. Some contradictory data exists for hydrothermal systems in the
423 deep ocean (Ref. 35 and references therein), but no deep vents exist in the MED.
424 Hydrothermal systems in shallow (less than 200 m-depth), near-shore environments
425 have been largely ignored, and their contribution to the global Hg cycle remains
426 unknown¹³. In the MED several shallow sites are known (e.g., Milos). A first
427 investigation of the Panarea site (Italy) shows significant Hg inputs, especially Hg⁰ (Ref.
428 36). The study finds that the Hg⁰ evasion flux is negligible in the MED budget. The
429 authors state that previous assessments of total hydrothermal inputs to the MED ~15 Mg
430 y⁻¹ (Refs. 40, 41), are underestimations. This possibly important source is far from being
431 well-constrained; obviously, more data are crucially needed in this field.

432 ***2.6. Riverine and submarine groundwater discharge***

433 According to a recent paper, riverine discharge from European rivers into the MED is
434 2.9 Mg y⁻¹ (Ref. 120); this input is highly seasonal due to the Mediterranean
435 hydrological regime⁷⁵. However, the inputs from rivers into the eastern and southern
436 parts of the MED shore are not included in this inventory. The way we have chosen to
437 assess the total Hg riverine influxes to the MED is by extrapolating the mean Hg
438 concentrations (2.45 pmol L⁻¹, 0.85 nmol g⁻¹, for dissolved and particulate Hg,
439 respectively) of the Rhône River, for which multi-year time-series exist⁴³, to the total
440 MED river discharge. We arrive at a total Hg input of 6 Mg y⁻¹, which is divided into 2.3
441 and 3.7 Mg y⁻¹ for the Western and Eastern basins, respectively. Hydrological data used
442 for these calculations are from Refs. 121, 122, 123. These calculated fluxes are in the
443 same order of magnitude that the Hg accumulated annually in shelf sediments (see
444 Section 2.3.). This observation suggests that most of the Hg associated with riverine
445 particles settles into shelf sediments.

446 For submarine groundwater discharges (SGD) the available data are even more
447 limited. The Hg load of SGD has been studied in the Marseille region (NWMED): THg
448 concentrations were in the picomolar range and often $< 3 \text{ pmol L}^{-1}$ (Ref. 124). For a 20
449 km long coastline an annual mean of THg discharge of $0.14 \pm 0.12 \text{ kg}$ was calculated.
450 Extrapolating this figure to the total MED shoreline and assuming constant submarine
451 discharge point and flux density gives a total Hg flux from SGD of $\sim 0.32 \text{ Mg y}^{-1}$.
452 However, this figure could be largely underestimated. Trace element SGDs in the
453 WMED have been estimated to be roughly in the same range as riverine discharges¹²⁵.
454 Assuming a similar behavior for Hg would give a total Hg discharge from submarine
455 groundwaters an order of magnitude higher, namely $\sim 6 \text{ Mg y}^{-1}$. In summary, Hg inputs
456 from continental exoreic water sources to the MED can be estimated at ca. 12 Mg y^{-1} .
457 Here again, this flux is not well constrained, and more studies are needed on rivers and
458 especially SGD.

459 *2.7. Mercury budget in the Mediterranean Sea*

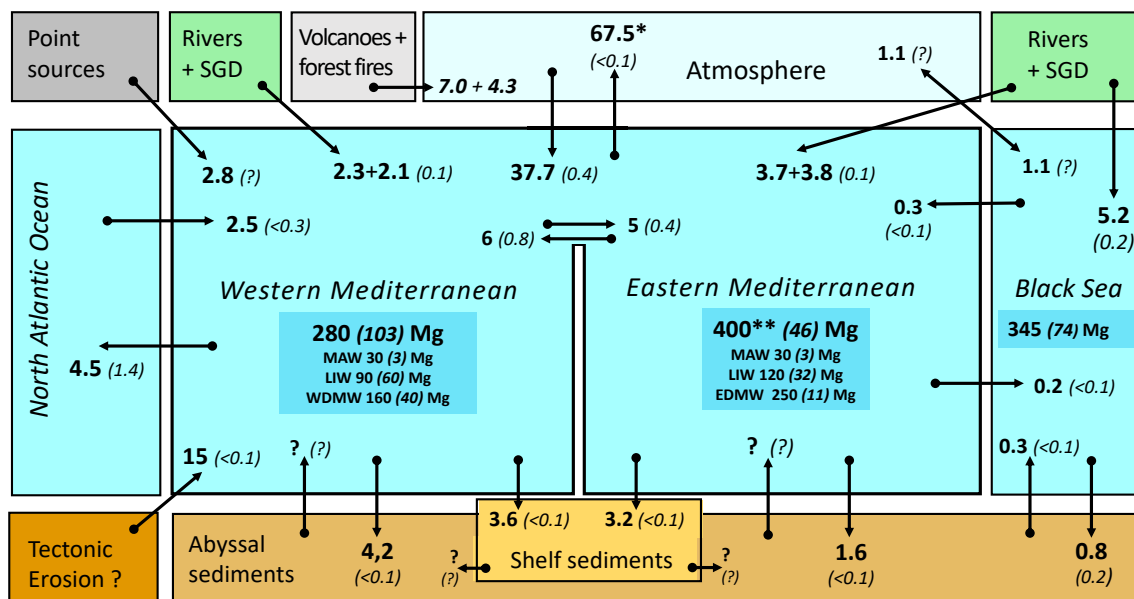
460 The diagram in Figure 6 sums up the Hg exchanges at the boundaries of the system and
461 the Hg species inventory of the two MED basins. Precision concerning the Hg
462 measurements, their natural variability, as well as that of the hydrodynamic and
463 particulate fluxes, make this an exercise with major uncertainties. However, information
464 that can be gained by such a mass balance calculation is to reveal the relative
465 magnitudes of various sources and sinks and to test the hypothesis of a steady-state of
466 Hg in the MED waters. In terms of balance, Hg output exceeds input by $\sim 15 \text{ Mg y}^{-1}$,
467 which is $\sim 17\%$ of the total export flux. Considering the uncertainties, the present Hg
468 budget is close to balance. However, if we consider the excess of Hg export as real, this
469 means that the Hg quantity in the MED is decreasing at the time scale of the residence
470 time of Hg ($2 \% \text{ y}^{-1}$). This is consistent with the observations of a $\sim 30\%$ decreasing Hg
471 concentrations in the MED over the last 20 years⁴⁶.

472 In summary, the achievements of the updated budget are:

- 473 – It is confirmed that the exchanges between surface water and the atmosphere
474 dominate the Mediterranean Sea Hg transport; however, the excess of evasion
475 compared to the deposition, currently given by the models, is still insufficiently
476 supported by the observations to be fully reliable;

- 477 – In absence of a robust quantification of diffusive Hg flux from sediment, the Hg
478 buried in deep sediment is estimated around 5.8 Mg y⁻¹;
- 479 – The rate Hg accumulated in shelf sediments is ~6.8 Mg y⁻¹, which is similar to
480 the Hg flux from rivers; part of it is probably temporarily trapped in coastal
481 sediments before a possible transfer to the deep sea *via* submarine canyons;
- 482 – The finding that Hg efflux to the Atlantic Ocean, with intermediate and deep
483 waters at Gibraltar, dominates the Atlantic input in surface water (by a factor
484 ~2), with Hg entering the MED as inorganic species and escaping substantially
485 as MeHg; MED is a site of MeHg production and a point source of MeHg for
486 the adjacent Northeastern Atlantic Ocean (~1.4 Mg y⁻¹);
- 487 – The estimation of a Hg (MeHg) content of the MED ~680 Mg (~150 Mg), with
488 0.7 % being associated with biota (6 % of which is annually removed by
489 fisheries) (see section 4 below);
- 490 – The estimation of a residence time of Hg in MED waters < 10 years, which is
491 roughly 5 to 10-times less than the residence time of waters; thus, decreasing
492 the atmospheric Hg deposition (i.e., a decrease of anthropogenic emissions)
493 over the MED region would more rapidly decrease the Hg concentration in
494 MED waters than in other parts of the World Ocean.

495 The present budget remains poorly constrained about several Hg inputs especially
496 those from geotectonic origins, coastal erosion, SGD, sedimentary mobilization, and
497 point sources. These uncertainties are added to that of the imbalance in the Hg air-sea
498 exchanges between evasion and deposition. Seasonal variation of numerous inputs needs
499 to be assessed. In addition, the transport of particulate Hg inputs from terrigenous origin
500 to the deep open sea through canyons is not quantified. For example, which part of
501 riverine Hg inputs (associated with particulate material) remains in the margin
502 sediments, which part reaches the abyssal sediments *via* canyons or is released in the
503 water column, and may become available to benthic food webs? Such questions need
504 answers for refining the Hg budget in order to use it to manage the near-shore areas
505 where fishing and aquaculture activities are located.



506

507 **Figure 6.** Total Hg (THg in bold) and methylated Hg (MeHg in brackets) annual mass fluxes in
 508 the Mediterranean Sea (Mg y⁻¹). In the dark blue rectangle are the Hg inventories (Mg) in sub-
 509 basins and water masses. Fluxes from modeled air-sea exchanges are discussed in Section 2.1,
 510 Gibraltar exchanges are from Section 2.4, volcanic inputs from Section 2.5, and sediment
 511 deposition from Section 2.3; point sources are taken from Refs. 32, 33, 40, and 126; tectonic
 512 fluxes from Ref. 40 (probably an underestimation), are not differentiated according to basins;
 513 erosion fluxes are not quantified; fluxes from/to the Black Sea are from Ref. 45. The seawater
 514 fluxes at the Sicily Strait are from Ref. 123. Mediterranean areas and volumes are from Ref.
 515 127. *Range: 50-100 Mg y⁻¹; **THg concentrations in the EMED used for calculation are
 516 limited to 24 measurements on only one profile in the Ionian Sea acquired in 2004 during
 517 MEDOCEANOR-3 cruise.

518

519 3. Biological mercury transformations: state of the art for MED

520 The net amount of MeHg formed in the ocean is controlled by three processes: (i) the
 521 methylation of Hg_i^{II} to MMHg, (ii) MMHg demethylation to Hg_i^{II}, and (iii)
 522 interconversion between DMHg and MMHg. Abiotic methylation of Hg_i^{II} is possible if
 523 suitable methyl donors are present, but research efforts have mostly been concerned with
 524 biologically mediated Hg methylation. The biological methylation of Hg_i^{II} to MeHg can
 525 be performed by microorganisms carrying the *hgcA* and *hgcB* gene clusters^{128, 129, 130, 131}.
 526 A detailed description of the gene clusters is given in Supporting Information (SI.5).
 527 Some *Nitrospina hgcA*-like genes in one of three MED water samples were also
 528 detected¹³². In particular, those gene copies were detected in surface waters and were not
 529 detected at the deep chlorophyll maximum of the MED. Three samples are not
 530 representative of the vertical and horizontal variability of the MED but, based on previous
 531 knowledge, it can be speculated that *hgcA* might be more abundant in surface waters and

532 at the OMZ of the MED. Due to the lack of data, a more extensive evaluation of the
533 presence and activity of *hgcA* in the MED is needed to determine the position in the water
534 column where these microorganisms are active, and thus responsible for biological
535 MMHg formation in the MED water column, and to unveil their different metabolic
536 capacities.

537 Besides the occurrence of potential Hg_i^{II} methylators in the ocean, the amount of
538 Hg_i^{II} available for methylation plays an important role in determining the rate of this
539 process. In this context, Hg_i^{II} reduction, which might decrease Hg_i^{II} bioavailability for
540 methylation, and MMHg demethylation, which might increase it, are both critical
541 processes to consider. Both Hg_i^{II} reduction and MMHg demethylation can be biotically^{133,}
542 ¹³⁴ and photochemically mediated^{135, 136, 137, 138}. As mentioned above, although rates of
543 photochemical transformations have never been reported for the MED, it is logical that
544 these processes are limited to the photic zone and thus to the AW. Similarly, there is no
545 information concerning biological Hg_i^{II} reduction. Two pathways of MMHg
546 demethylation have been identified: an oxidative pathway yielding Hg^{II} and CO_2 , and a
547 reductive pathway yielding Hg^0 and CH_4 . Since the Hg^0 produced from reductive
548 demethylation can diffuse out of the cell, it has been proposed that reductive
549 demethylation is a cellular detoxification mechanism¹³⁴, which would dominate at high
550 Hg concentrations, whereas the oxidative pathway, which is an unknown, would be more
551 important at low Hg concentrations¹³⁹. MMHg demethylation is biologically mediated by
552 the *mer* operon^{134, 140}. Lastly, the interconversion between DMHg and MMHg is still
553 poorly understood but has been suggested to be potentially abiotic^{141, 142}. In the MED the
554 lack of knowledge regarding metabolic pathways and the organisms involved in these
555 processes has limited the possibilities to further understanding of Hg biogeochemical
556 cycling.

557

558 **4. Biological transfers in food webs**

559 In the MED, top-predator fish often exceed EU regulatory Hg thresholds^{75, 143, 144, 145, 146,}
560 ^{147, 148} and contribute to the increase in MeHg exposure of seafood consumers^{10, 149}. Also,
561 for over 50 years, Hg-enrichment in Mediterranean fish compared to other oceanic
562 regions at the same latitudes has been observed (e.g., Refs. 17, 18, 148), with the result
563 that Aston and Fowler²⁰ describe these findings as a real “mercury enigma” in MED
564 biota. After debates about the possible importance of biological factors^{20, 75}, a comparison

565 of Hg content in hake and its food web elements from the MED and the adjacent North
566 Atlantic Ocean suggests a multi-causal explanation for this issue²¹, namely (i) the
567 location of the MeHg maximal concentration in the water column, (ii) the growth rates of
568 the fish, and (iii) the structure of the food webs.

569 Most available information on Hg concentrations in Mediterranean organisms, from
570 primary producers to marine mammals and birds, recorded between 1969 and 2015 was
571 compiled into a large database¹⁴⁸. Among Animalia about 80 % of samples concern
572 Actinopterygii (mainly teleost fish) and Bivalvia (mainly mussels), while among Plantae
573 87 % of the data concern the seagrass *Posidonia oceanica*, highlighting the lack of
574 knowledge on Hg content in important small organisms, such as phytoplankton
575 producers, zooplankton consumers, and benthic invertebrates. More information is
576 available from the northern than the southern part of the MED and the western rather than
577 the eastern basin¹⁴⁸. Hg transfer in biota involves three complex multifactorial processes
578 (bioconcentration, bioaccumulation, and biomagnification) interacting at different levels
579 of the food webs, which need to be taken into account for a true understanding of
580 Mediterranean specificities and to facilitate geographical comparisons.

581 **4.1. Bioconcentration**

582 Bioconcentration is the absorption of contaminants in organisms directly from water
583 through cell membranes. This is the first and most important step in Hg transfer, which
584 occurs mainly at microorganisms levels. Bioconcentration depends not only on the
585 bioavailable Hg concentration in seawater, but also on the specific composition of
586 phytoplankton communities, their abundance, and size, which govern Hg sorption and
587 uptake in the first trophic level of food webs¹⁵⁰. It has been demonstrated that MMHg is
588 preferentially integrated into the cell cytoplasm whereas Hg_i^{II} is adsorbed on
589 phytoplankton membranes¹⁵¹. As a consequence, MeHg is assimilated by zooplankton
590 four times more efficiently than Hg_i^{II} (Ref. 150). For a given Hg concentration in
591 seawater, absorption is negatively related to phytoplankton abundance (dilution by
592 biomass), and uptake is negatively related to cell size (higher surface/volume ratio in
593 smaller cells) and their rates vary among species^{152, 153}. As the base of the food web is
594 mainly made up of pico- or nano-bacteria and phytoplankton in oligotrophic
595 Mediterranean seawaters¹⁵⁴, the combination of low phytoplankton abundance and small-
596 sized cells increase both sorption processes resulting in higher Hg concentrations of the
597 first trophic level in the MED than in the northeastern Atlantic²¹. At a smaller spatial

598 scale in the MED, higher Hg bioconcentration in phytoplankton is also found in
599 oligotrophic offshore waters than in mesotrophic coastal waters due to similar
600 processes²¹. In the MED, the higher proximity at mid-depth of both chlorophyll (~40
601 m)¹⁵⁵ and MeHg maxima (~250-400 m)²¹ increases Hg bioavailability for phytoplankton
602 incorporation. In contrast, these two zones are more separated in the Northeastern
603 Atlantic, where the MeHg maximum is located in deep waters (800 m)²¹ and the
604 chlorophyll one in shallow waters (5-40 m), contributing to reduce bioconcentration at
605 the base of the food webs in this region. In the Black Sea, MeHg maximum occurs in
606 permanently anoxic waters⁴⁵. The strong stratification of the water column between the
607 oxic and anoxic layers precludes the exposure of higher living organisms to elevated
608 MeHg concentrations. In addition, the high primary production of the Black Sea adds a
609 bio-dilution effect and may contribute to explaining the lower Hg bioconcentration
610 observed¹⁵⁶.

611 Studies in the Gulf of Lion provide evidence of higher Hg concentrations in the
612 smaller (6-60 μm), rather than the larger (60-200 μm), phytoplankton fractions
613 analyzed¹⁵⁷, consistently with the results obtained experimentally and by modeling¹⁵⁰,
614 ¹⁵⁸. However, in these small-size fractions, detrital organic particles and numerous
615 associated bacteria are mixed with autotrophic and heterotrophic plankton. That raises
616 the question of the relative role of living and non-living particles, and of the different
617 types of plankton in Hg transfer in food webs. Which species or size fractions are the
618 most significant for Hg transfer in food webs? It seems that Hg could be more readily
619 assimilated by copepods when they are feeding on ciliates (protozoa) than on
620 phytoplankton or heterotrophic dinoflagellates¹⁵⁹.

621 **4.2. Bioaccumulation**

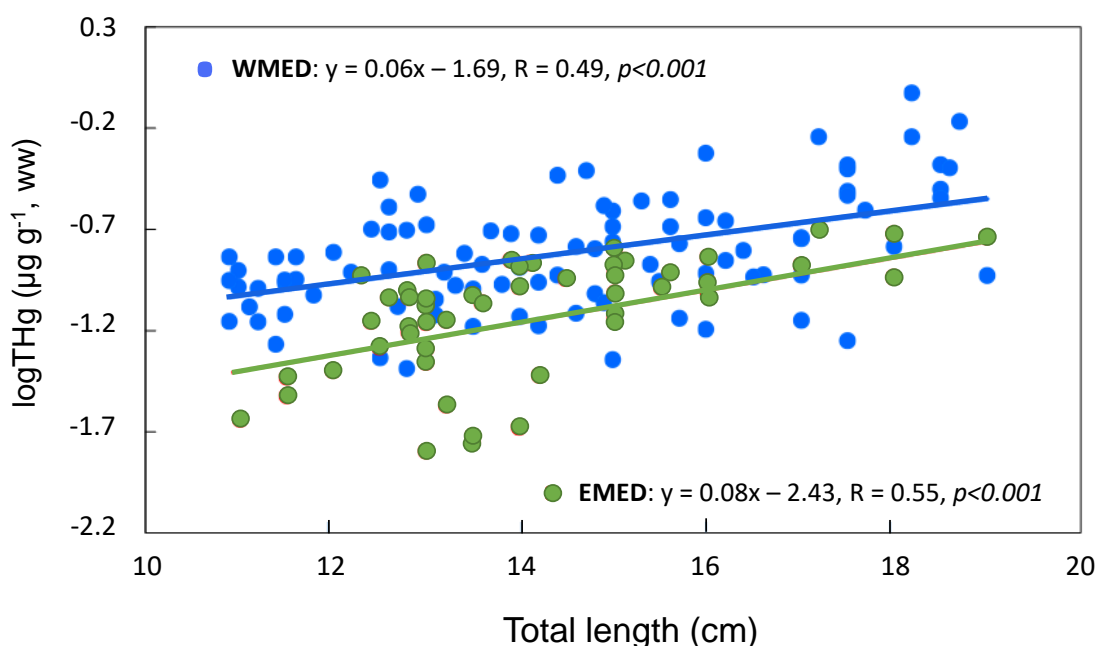
622 Bioaccumulation refers to a contaminant increase in an organism during its lifetime from
623 both the environment and food consumption. Hg bioaccumulation in consumer organisms
624 during their lifetime is mainly due to prey consumption^{160, 161}, and differs widely
625 according to species, and the organs or body parts considered^{148, 157, 162}. Thus, the Hg
626 content of prey is one of the major parameters for explaining bioaccumulation in
627 organisms, and a positive correlation between Hg content in food and consumer is
628 generally observed¹⁶³. In the MED as elsewhere, whole organisms are analyzed for
629 plankton, benthic invertebrates, and fish larvae due to their small size, whereas muscle
630 tissues are generally analyzed in larger marine consumers (crustaceans, cephalopods, and

631 fish) due to their consumption by human populations^{10, 146}. Other tissues are analyzed for
632 larger Mediterranean predators, such as skin biopsies for mammals¹⁶⁴ or blood for
633 seabirds¹⁶⁵. Higher Hg concentrations are generally found in the liver, compared to
634 muscle and the gonads in MED fish^{157, 166, 167}, while this pattern may differ according to
635 species, higher Hg content is found in muscle than liver of hake¹⁶⁸ and shark¹⁶⁹.
636 Conversely, a higher MeHg percentage (85-97 %) is recorded in muscle than in the liver
637 (30 %)¹⁶² due to the slower elimination rate from muscle than liver (2 % and 60 %
638 respectively)¹⁶⁷. In addition to organ differences, bioaccumulation is modulated at the
639 individual level by a series of interacting biological (species, size, weight, sex, age, life
640 duration, growth rate, reproduction, metabolism, proximal composition, detoxification
641 mechanisms, diet, etc.) and environmental (depth, habitat, temperature, primary
642 production, etc.) factors, as described in studies of the European hake *Merluccius*
643 *merluccius*^{21, 170, 171} and small pelagic fishes in the Gulf of Lion¹⁵⁷. The synergistic and
644 antagonistic effects of all these factors, which vary in space and time for a given species,
645 explain the high variability of the vast amount of data published on Hg concentrations in
646 MED organisms and the complexity of fully understanding and explaining local and
647 regional differences (e.g., Ref. 148 and references therein). Generally speaking, a positive
648 correlation is observed between Hg concentration and individual size, weight, age,
649 trophic level and depth, and a negative correlation with growth rate (Hg dilution by an
650 increase in organism biomass) in MED fishes and mammals, with numerous exceptions
651 according to species or populations. For example, a higher Hg content was found in male
652 than female hakes of similar size in the Gulf of Lion but not in the Bay of Biscay, as
653 males grow more slowly than females in the MED, but not in the Atlantic²¹. Hg content
654 was correlated with size in *Mullus surmuletus* in the Ligurian Sea¹⁷² and south of Spain¹⁶⁸
655 but not in the Gulf of Lion¹⁵⁶. A recent study also demonstrates the importance of the
656 proximal composition (mainly protein and lipid contents) of organisms on Hg
657 concentration in MED fish¹⁶⁸. Besides, as the whole life history determines Hg
658 accumulation in organisms, the inter-individual variability would be higher in the older,
659 often also the larger, individuals in a population, a pattern observed in MED fishes^{170, 173}
660 and marine mammals¹⁶⁴. Most authors agree however on the higher Hg bioaccumulation
661 in MED benthic fish species compared to pelagic fish, and in individuals within species
662 occurring at deeper than in shallower waters^{166, 173, 174, 175, 176}, while exceptions are also
663 observed¹⁷⁷.

664 Regional comparisons of Hg concentrations in marine organisms are thus
665 complicated by the combination of the high number of factors involved in contaminant
666 bioaccumulation and may differ according to the organisms studied¹⁷⁸. Mediterranean
667 organisms, from sponges to fish, marine mammals, and seabirds, are known for their
668 higher Hg concentrations than their Atlantic counterparts^{21, 48, 164, 165, 179, 180, 181, 182}. Within
669 the MED, some geographic regions such as the North Adriatic Sea, the Tyrrhenian Sea,
670 and the Sea of Marmara^{174, 180, 181} are known hotspots for Hg bioaccumulation, while the
671 Aegean Sea¹⁸³, Ionian Sea¹⁷⁴, the Black Sea¹⁵⁶, and the Tunisian coast¹⁶² appear to be less
672 contaminated. Locally, Hg concentration in one species may vary by an order of
673 magnitude, as observed for mussels on French MED coasts¹⁸⁴. The exceptionally high
674 spatial variability in MED organisms is highlighted by all studies, both between western
675 and eastern basins, northern and southern coasts, and among habitats and depths. An
676 example of the WMED-EMED difference of Hg content in fish is provided by the red
677 mullet *Mullus barbatus*, a much-used species in monitoring surveys, from the Gulf of
678 Lion¹⁷⁰ and the coast of Turkey¹⁸³. *M. barbatus* of the same size range (11-19 cm TL)
679 exhibit a ~2 times higher mean Hg content in the WMED ($0.190 \pm 0.013 \mu\text{g g}^{-1}$ wet
680 weight in muscle, n = 94) than the EMED ($0.090 \pm 0.017 \mu\text{g g}^{-1}$ ww, n = 52) (Fig. 7). The
681 regression $\log\text{Hg}$ vs size presents a significantly higher intercept in the WMED than in
682 the EMED, suggesting a higher Hg concentration at the base of the food web in WMED,
683 while slopes do not differ due to the high variance of data indicating similar Hg
684 bioaccumulation rates in the two fish populations. Such regional differences in fish Hg
685 content could be related to the higher MeHg concentration in WMED than EMED waters
686 (Fig. 3), which could induce more pronounced bioconcentration processes and thus
687 higher Hg content in all trophic levels in WMED food webs. Consistently, the relatively
688 high Hg bioaccumulation observed in Mediterranean hakes²¹ could be essentially related
689 to the environmental specificities of the MED compared to the adjacent NE Atlantic,
690 including slightly higher MeHg concentrations in waters where predators are foraging.
691 This latter hypothesis is supported by recent results on bluefin tuna, for which very high
692 Hg levels have been observed²². Indeed, Tseng et al. (2021)²² showed that this long-lived
693 apex predator has Hg accumulation rates (defined as a change in muscle Hg concentration
694 per unit change in either size/weight or age) which reach the highest level in the MED
695 and decrease as North Pacific > Indian Ocean > North Atlantic. The authors argue that the
696 Hg accumulation rate in tuna can be used as a Hg contamination index in the oceans. This

697 interesting hypothesis deserves further testing and it is probably related to the high
698 methylation capacity of MED waters (see section 2.2.2).

699 In addition, the higher temperature of the MED and its oligotrophic waters would
700 induce an increase in metabolic activity^{185, 186} and a decrease in the growth of the
701 organisms^{187, 188}, leading to a smaller size at a given age, which, along with a lower Hg
702 elimination rate¹⁶⁷, would induce higher bioaccumulation of Hg in Mediterranean
703 organisms^{21, 48}.



704

705 **Figure 7.** Log-log relationships between THg and total length in the red mullet (*Mullus*
706 *barbatus*) from the Gulf of Lion, France (WMED) and the Gulf of Izmir, Turkey (EMED).

707 **4.3. Biomagnification**

708 Biomagnification is defined as the increase in Hg concentration in organisms from prey
709 to predator throughout food webs from primary producers to high trophic level predators.
710 Some studies provide data on Hg biomagnification along Mediterranean food webs from
711 primary producers to various consumers at different trophic levels^{21, 157, 176, 178}. Most often
712 the food webs analyzed were comprised of only a few trophic levels as highlighted in the
713 worldwide meta-analysis¹⁸⁹ in which the food webs analyzed ranged across a mean of
714 only 1.7 trophic levels, but a few studies recently analyzed entire food webs from
715 phytoplankton to marine mammals¹⁵³. All studies provide evidence of an exponential

716 increase of total Hg concentration with the trophic level increase, and a steeper slope for
717 MeHg which presents a higher retention efficiency due to its lower elimination rate.

718 Mercury biomagnification in food webs is generally quantified either by the trophic
719 magnification slope (TMS) (also called biomagnification power), corresponding to the
720 slope (b) of the regression between logHg or logMeHg vs trophic level or $\delta^{15}\text{N}$ of the
721 organisms, or by the trophic magnification factor (TMF) calculated as $\text{TMF} = 10^b$ (see
722 Ref. 190 for a critical discussion). Trophic magnification slope generally ranges from
723 0.11 to 0.22 for total Hg and 0.14 to 0.36 for MeHg in the food webs studied from polar
724 to tropical ecosystems, which corresponded to TMFs ranging from 1.29 to 1.66 for Hg
725 and from 1.38 to 2.29 for MeHg^{153, 184, 189}. The TMFs calculated for Hg in Mediterranean
726 food webs are within this range with a lower value in Sicily (1.22, Ref. 175) than in the
727 Gulf of Lion (1.68, Ref. 171) or the Bay of Marseille (1.25 - 1.58, Ref. 177), but reaches
728 2.40 (TMS = 0.38) for MeHg in the Gulf of Lion²¹. A higher biomagnification power for
729 MeHg was calculated in the hake food web in the MED than in the NE Atlantic (2.40
730 and 1.95 respectively)²¹, while no difference in MeHg biomagnification power between
731 the MED and the Atlantic was found for deeper fish species occurring in deeper
732 waters⁴⁸, such as the sharks *Scyliorhinus canicula* and *Galeus melastomus*. Currently,
733 due to the scarcity of relevant data, it is not possible to account for a particular Hg
734 biomagnification in MED food webs. However, a possible hypothesis is that the smaller
735 size of individuals in the MED induces longer or more complex food webs, which may
736 result in a higher Hg biomagnification factor. It is proposed that longer food chains
737 induce a decrease in energy transfer and an increase in contaminant retention^{191, 192}.
738 During summer, when nutrients become limiting, changes in trophic conditions could
739 modify the importance of the microbial loop as well as the role played by mixotrophic
740 organisms in the trophic transfer of Hg. It is not known if there are differences in the
741 processes involved in Hg transfer and biomagnification in pelagic and benthic-
742 dominated food webs or a difference in the magnitude of similar processes. Few data are
743 available on Hg and MeHg concentrations in the benthic invertebrates which constitute
744 important prey sources for higher trophic level consumers. The specificity of the MED
745 food web functioning itself may well influence Hg transfer¹⁹³.

746 The use of different trophic markers (carbon and nitrogen stable isotopes, fatty acids,
747 amino-acids, compound-specific stable isotope analyses) and stable Hg isotopes may
748 improve the comprehension of trophic transfer in the first levels of the food web and

749 thus refine the estimation of Hg and MeHg transfers under varying environmental
750 conditions. Ecosystem models such as ECOPATH with ECOSIM, ECOSPACE, and
751 ECOTRACER^{194, 195} take into account all food web interactions. Applying such models
752 here should allow better quantification of the trophic transfers of Hg and MeHg in MED
753 ecosystems and their temporal and spatial variability. Regional food web models
754 accounting for bioaccumulation need to be implemented to simulate the spatial
755 variability, as well as the population-variability, of Hg concentration in organisms, and
756 refine the estimation of total Hg and MeHg content in MED biota. All these questions
757 require accurate knowledge of organism biology, physiology, and ecology, to determine
758 how they differ in the MED from adjacent areas.

759 ***4.4. Quantification of Hg content in Mediterranean biota and fisheries harvest***

760 From the data compiled in the Supporting Information (SI.6), we estimated the THg and
761 MeHg content in MED biota. Detailed methodological and calculation details are also
762 given in the Supporting Information (SI.7). The estimate indicated that MED marine biota
763 contains ~ 4.7 Mg of THg and ~2.2 Mg as MeHg. Due to the uncertainty associated with
764 the initial biomass estimation, a range between 3.0 and 6.4 Mg of THg in MED biota can
765 be approximated using the standard deviation of the biomass compartments¹⁹⁶. These
766 results illustrate not only the importance of primary producers, which represent 13 % of
767 THg in MED biota, as already observed in other mass balance inventories¹⁹⁷ but also the
768 chief importance of the benthos, a too often neglected compartment, which accounts for
769 ~50 % of THg (32 % of the MeHg) in MED biota. Cetaceans also constitute an important
770 Hg reservoir (10 % of THg and 18 % of the MeHg present in MED biota). However, THg
771 in biota represents only a small part (0.7 %) of the general Hg budget in the MED. An
772 estimation of Hg removed from the MED by fishery catches was performed using the
773 observed data of catches for the year 2011¹⁹⁶. A total of 0.30 Mg THg y⁻¹ and 0.26 Mg
774 MeHg y⁻¹ is extracted from the MED by fisheries, which is similar to the value of 0.29
775 Mg MeHg y⁻¹ calculated by Žagar et al.⁴¹ using a different method. However, in contrast
776 to these authors, total aquaculture products were not included in our estimation, which
777 could therefore be considered as a minimum value. Catches therefore annually remove ~6
778 % of the THg and ~12 % of MeHg held in living biomass in the MED. Sharks and small
779 pelagic fishes (including sardine and anchovy) constitute the main quantities of MeHg
780 (20 % each) removed by MED fisheries, followed by large pelagic (13 %) and large

781 demersal (11 %) fishes. These estimations should be treated with caution as a large
782 degree of uncertainty is associated with all steps of the calculations.

783

784 **5. Human exposure**

785 Mercury is one of the ten most important pollutants of global concern for human
786 health¹⁹⁸. The major toxic effects of MeHg, a naturally occurring organic form of Hg
787 prevalent in fish, are on the central nervous system, with the developing fetus being
788 most vulnerable¹. Consumption of fish is considered a major source of Hg exposure to
789 Europeans. Other sources are well described, but their contributions are minor in
790 comparison with fish consumption¹⁹⁹.

791 Human exposure to mercury and its compounds can be assessed through the
792 measurement of Hg concentrations in many different biological sample types. The most
793 commonly used biomarkers are the concentrations of mercury in hair, urine, blood, and
794 cord blood, and their selection can depend on factors such as the potential source of
795 exposure, chemical form, and exposure life stage. An extensive recent review indicated
796 that the individuals with the highest reported Hg levels were those living in the Arctic,
797 Pacific, MED, and Atlantic coast regions who consume the highest amounts of fish,
798 seafood, and marine mammals²⁰⁰. It has been shown that several species of fish from the
799 MED have higher levels of Hg in their tissues compared with the same species from the
800 Atlantic Ocean^{201, 202}, and references cited in section 4.3. An extensive review of
801 mercury levels in biota is presented by Cinnirella et al.¹⁴⁸ and indicates that among all
802 the species considered, *Diplodus sargus*, *Sardina pilchardus*, *Thunnus thynnus*, and
803 *Xiphias gladius* show trends of mercury concentration higher than safe limits defined by
804 WHO and EU.

805 Human exposure to Hg in Europe, and in particular, the question of whether MED
806 populations are more exposed to this contaminant than other European populations has
807 been addressed in the literature. Two studies have evaluated Hg concentrations in blood,
808 urine, and hair, widely used biomarkers to evaluate Hg human exposure, of populations
809 from European Countries^{199, 203}. Both studies agreed on the fact that there are significant
810 differences in MeHg exposure across the EU and that exposure is highly correlated with
811 the consumption of fish and marine products, as well as the availability of large fish
812 species from the MED. Whether human exposure to Hg is higher in the MED than in

813 North European countries still needs to be elucidated through a well-designed
814 comparative study.

815 The results of studies in the MED countries are provided in the Supporting
816 Information (SI.8)^{199, 203}. The highest levels are found in coastal regions with local
817 seafood consumption (Spain, Morocco, Tunisia, and Greece) which is consistent with
818 other studies around the world. In the framework of the EU-funded DEMOCOPHES
819 project²⁰⁴, the dietary habits and consumption frequency of fish and other marine
820 products showed great variations among the 17 EU countries, which was also reflected
821 in the high variability of Hg levels in the hair of mothers and children. Among the MED
822 countries participating in DEMOCOPHES the highest values (geometric means) were
823 found in Spain ($1.59 \mu\text{g g}^{-1}$), whereas Cyprus and Slovenia showed much lower values
824 ($0.43 \mu\text{g g}^{-1}$ and $0.26 \mu\text{g g}^{-1}$, respectively).

825 In the MED region, two cohort studies aimed to link prenatal Hg exposure and
826 health outcomes in newborns. The prenatal exposure in both studies was based on cord
827 blood mercury measurements. In Spain, the “Environment and Childhood” (INMA) study
828 implemented in the period 2004 to 2008 included several regions, and 1883 cord blood
829 samples were analyzed for THg²⁰⁵. The highest concentrations expressed as geometric
830 means were found in samples collected in Valencia ($9.5 \mu\text{g L}^{-1}$) and Asturias (10.8 ng mL^{-1})
831 and were strongly related to fish consumption, especially large oily fish and tuna.
832 The second MED cohort study included coastal regions in Italy, Slovenia, Croatia, and
833 Greece^{206, 207} in the period between 2007 and 2011. This cohort study included 1308
834 mother-child pairs enrolled in the Public Health Impact of long-term, low-level, Mixed
835 Element exposure in a susceptible population (PHIME). The highest levels of cord blood
836 samples were found in the Greek population with geometric means of 7.7 ng mL^{-1} ,
837 followed by Italy with 5.6 ng mL^{-1} , Croatia with 5.1 ng mL^{-1} , and the lowest in Slovenia
838 with 2.1 ng mL^{-1} . These levels were strongly correlated with fish consumption, and in
839 Greece primarily due to locally caught fish. The Valencia and Asturias region in the
840 INMA and Greek PHIME prenatal exposure values are comparable to regions with high
841 fish intake in Japan, Honk Kong, Korea, and Polynesia²⁰⁵. These two studies confirm the
842 data presented in Supporting Information (SI.8) that indicate high variability of Hg
843 exposure in the MED region reflecting variation in the frequency of fish consumption,
844 their sources, and type. Similar findings were reported in a recent publication of Petrova
845 et al.¹⁰, where mean Hg levels in hair for women of childbearing age on the French

846 Mediterranean coast were higher than for women of childbearing age from other
847 European countries. This trend is in accordance with the higher annual fish consumption
848 *per capita* in various European countries. Besides, it has to be noted that fish from
849 aquaculture often have lower Hg levels compared with wild fisheries. For example,
850 levels of Hg in seabass (*Dicentrarchus labrax*) from wild fisheries in the MED were, on
851 average, approximately 10 times higher than in aquaculture seabass²⁰⁷.

852 While fish consumption is an important element of human health, especially in the
853 early stages of life^{208, 209}, higher MeHg exposure during pregnancy is associated with a
854 poorer metabolic profile. Both MED epidemiological studies, INMA and PHIME, also
855 indicated that there is a growing awareness of inter-individual differences in the
856 toxicokinetics of mercury and the resulting biomarker measurements may be influenced
857 by genetic polymorphisms^{210, 211}. Since the symptoms of MeHg exposure are subtle and
858 multi-causal, there is still no consensus on a health-based guidance value for MeHg
859 exposure despite the large number of studies trying to connect low exposure levels to
860 actual risk^{209, 212}. However, there is a general recommendation that pregnant women,
861 children, and women of childbearing age should be protected as much as possible from
862 Hg exposure. Therefore, it is important to know what the actual exposure to MeHg is in
863 the general population and what the sources of exposure are to formulate adequate
864 mitigation strategies and recommendations. For example, an attempt was made for the
865 Italian population²¹³ with the formulation of advice regarding food habits that could
866 maximize the benefits, whilst reducing the risks of MeHg intake in sensitive groups
867 without compromising seafood consumption. This should allow a better understanding
868 of the food risk associated with mercury, particularly in highly polluted sites. Overall,
869 the Minamata Convention on Mercury sets guidelines for limiting human exposure to
870 Hg. Article 22 of the Minamata Convention calls for parties to monitor mercury in the
871 environment as well as in people (biomonitoring) as a way of assessing the effectiveness
872 of the convention.

873

874 **6. Modeling the Hg cycle in the Mediterranean**

875 Numerical biogeochemical models are effective tools to investigate the fate and
876 transport of Hg in the environment. Synthesizing available knowledge into a rigorous
877 framework, they help to highlight gaps in process understanding and data availability^{32,}
878 ^{33, 45, 214, 215, 216, 217, 218, 219, 220, 221, 222, 223}. Moreover, models can be used to predict the

879 evolution of a system under different Hg emission scenarios, trophic conditions, and
880 climate change, supporting the evaluation of alternative management strategies^{218, 219, 224,}
881 ^{225, 226, 227}. Reviewing modeling studies for the marine Hg cycle in the Mediterranean
882 area, we found that only one paper has sought to model the Hg cycle in the MED at the
883 basin scale⁴¹, pointing out uncertainties in Hg input to the basin and a poor
884 understanding of Hg methylation and demethylation processes at that time. Other
885 modeling efforts in the MED are local scale studies focusing either on transport and
886 transformation processes of Hg species in regional seas⁶⁹ and coastal sites^{32, 224, 228, 229,}
887 ^{230, 231}, as well as on the bioaccumulation and biomagnification processes^{21, 232}. Most of
888 these models still presented several limitations, namely, the use of the quasi-steady state
889 approach, coarse spatial resolutions, and the lack of full coupling between physical and
890 biogeochemical processes.

891 Small-scale assessments are relevant to provide estimates of Hg fluxes from coastal
892 and former industrial areas²³³ since a comprehensive assessment of Hg point sources and
893 legacy Hg for the MED is lacking. However, existing modeling studies for Hg in the
894 MED are also geographically biased as they have been carried out in the areas where
895 more data have been collected over the years: either the Northern Adriatic Sea, or the
896 NWMed. Significant differences in the distribution and fluxes of Hg species are
897 observed^{46, 88}, in these two sub-basins, driven by contrasting oceanographic and
898 biogeochemical features, (i.e. the Northern Adriatic Sea is a shallow shelf with depth <
899 50 m and high river discharge, while the NWMed a deep system with seasonal
900 upwelling events), but a complete understanding of the MED system as a whole is
901 missing.

902 Remarkable research efforts in the last decades to unveil the mechanisms
903 underlying Hg methylation in the ocean pointed out organic matter remineralization as a
904 key process that triggers the release of dissolved Hg and fuels the activity of
905 heterotrophic bacterioplankton^{96, 97, 234, 235, 236}. Phytoplankton phenology patterns have a
906 large impact on MeHg production and bioaccumulation, as the cell size affects both the
907 ability to bioaccumulate Hg^{152, 158} and the sinking velocity after death, with small slow-
908 sinking plankton favoring water column Hg methylation in the water column^{91, 237}, and
909 large fast-sinking plankton acting as a fast vector for Hg sequestration through
910 scavenging and transport to the seafloor²³⁸. These pieces of evidence are fostering new
911 efforts aimed at developing integrated modeling tools that couple the biogeochemistry of

912 Hg species with that of organic matter and nutrients and with hydrodynamic transport²¹⁹,
913 ²²³. At the state of the art, coupled physical-biogeochemical models for the MED, can
914 simulate the key processes of nutrients (i.e., nitrogen, phosphorus, silica, iron) carbon,
915 and oxygen in the water, sediments, and in the food web from heterotrophic bacteria to
916 phytoplankton and zooplankton, reproducing the observed spatial gradient and seasonal
917 variations of chlorophyll and primary production at a spatial resolution up to 1/64
918 degree²³⁹. Validated model outputs for the BFM-OGSTM model, a biogeochemical
919 model coupled to the physical model NEMO-OceanVar, are freely available at the
920 Copernicus Marine Service site (<https://resources.marine.copernicus.eu>), with a spatial
921 resolution of 1/24 degree, for 125 depth levels, for forecast simulations and 20-year
922 reanalysis. Given the high standard attained in physical-biogeochemical models, a full
923 physical-biogeochemical-Hg coupling will likely add insights into the cycling of Hg in
924 the MED and its possible future evolution.

925 To improve our ability to model the Hg cycle, a better mechanistic understanding is
926 also needed. A few measurements are available for Hg methylation and demethylation
927 rates in the MED waters, as well as for the formation of Hg⁰ and DMHg^{43, 44, 240}; but
928 rates of photochemical transformations have never been assessed in the MED^{137, 138}, nor
929 has a full mechanistic understanding been achieved for any of these processes.
930 Moreover, a recent review highlighted significant uncertainties in assessing potential
931 seawater Hg methylation and demethylation rates²⁴¹. Given the relevance of DMHg in
932 the open ocean^{39, 43}, more observations and modeling experiments are needed to
933 constrain transformation kinetics between DMHg, MeHg, and inorganic Hg^{II} (Ref. 237).
934 Further investigation of Hg species transformations in sub-basins of the MED with
935 different trophic status could provide more reliable site-specific rates to be used in the
936 models and could help to elucidate how different controlling factors, such as primary
937 production, dissolved organic matter, oxygen, temperature, and chlorides affect
938 transformations kinetics. The continuous availability of data of Hg species in water and
939 plankton, the latter being particularly scarce in MED¹⁴⁸, is also crucial for model
940 validation and to improve our ability to deal with the challenges posed by climate
941 change.

942

943 **7. Overview of recent advances**

944 Compiling the oceanographically consistent THg data obtained in the open WMED
945 waters between 2000 and 2017 allowed us to draw a consistent pattern of Hg
946 distributions (Fig. 2). The THg concentrations of the upper layer (AW) are rather
947 variable (as a result of Hg evasion and biological pumping) averaging 0.86 ± 0.27 pmol
948 L^{-1} , whereas, in the intermediate and deep waters (EIW+WMDW), they are more
949 homogenous with a mean of 1.02 ± 0.12 pmol L^{-1} . In the EMED, the available THg
950 measurements are in the same range as those of the WMED but are far too few to
951 determine any consistent oceanographical pattern. MeHg represents around 10, 40, and
952 13 % of THg in AW, EIW, and DMW, respectively. The highest MeHg values are found
953 in the OMZ with high AOU (Fig. 4). The methylating, *hgcA*-like genes from different
954 microbial groups have even been identified in MED waters. The MeHg distribution
955 seems likely to be ultimately governed by the intensity of primary production and the
956 associated OM degradation. Consistently, MeHg concentrations in the mesotrophic
957 WMED average twice those in the oligotrophic EMED. In addition, the methylation
958 capacity of MED waters is high compared to other parts of the World Ocean. The THg
959 (MeHg) inventories in waters are ~ 280 (100) Mg and ~ 400 (50) Mg for the WMED and
960 EMED, respectively. Air-sea exchanges dominate the Hg fluxes, and Hg evasion largely
961 exceeds atmospheric deposition (~ 30 Mg y^{-1} net). However, the excess of evasion, given
962 by the models, is still insufficiently supported by the observations to be fully reliable.
963 The MED is a net exporter of Hg to the adjacent Atlantic Ocean (~ 2 Mg y^{-1} , with ~ 1.4
964 Mg y^{-1} as MeHg), and MED abyssal sediments are a net sink for Hg (~ 6 Mg y^{-1}),
965 whereas shelf sediments retain (at least temporarily) ~ 7 Mg y^{-1} . Most of this latter input
966 originates from rivers (~ 6 Mg y^{-1}). This budget is, however, still far from being well
967 constrained. For example, our estimations of submarine groundwater discharges, coastal
968 erosion, submarine tectonic inputs, and point sources are rather coarse. High Hg
969 concentrations were observed in Mediterranean predator organisms.

970 The MED is not only a bioreactor for MeHg production but also one of the places in
971 the World Ocean where the methylation capacity of the Hg is highest. The difference in
972 MeHg water concentrations between the MED basins (and other oceanic basins) appears
973 to be transferred through the food webs and the Hg content in predators to be ultimately
974 controlled by the MeHg concentrations of the waters of their foraging zones.
975 Mediterranean top-predator fish still exceed European Union regulatory Hg thresholds.
976 Since fish are the main vector of MeHg to humans, the current knowledge of the actual

977 exposure of MED populations to MeHg is still needed to formulate adequate mitigation
978 strategies and recommendations without compromising seafood consumption.
979 Mitigation of MED ecosystem exposure to Hg requires a full coupling of physical-
980 biogeochemical-Hg models based on a better assessment of anthropogenic Hg sources;
981 such coupling will likely add insights into the possible future evolution of the Hg
982 cycling in the MED, as a result of climate changes and variations in Hg atmospheric
983 deposition.

984

985 **8. Perspectives**

986 *8.1. Hg cycle, climate change, and human coastal management in the MED*

987 MED shares most of the uncertainties with other parts of the global ocean concerning the
988 Hg cycle and its possible modification due to climate change. Non-Mediterranean-
989 specific changes in Hg cycling are expected from climate change, such as those listed for
990 a global perspective²⁴², including changes in atmospheric Hg oxidation and deposition
991 and wildfires. Also, climate change is expected to induce modifications in the
992 hydrological regime that would consequently affect the Hg atmospheric wet depositions,
993 input regime from rivers, and submarine groundwater discharges. More specifically, the
994 MED is very vulnerable to future climate change scenarios²⁸, which are expected to
995 induce an increase in vertical stratification, a depletion of oxygen in deep layers, and a
996 reduction of primary productivity. Shallow and deep-water mixing would affect the
997 efficiency of Hg transfer to the bottom sediments. A possible decrease in plankton
998 productivity may slow down the uptake and subsequent Hg scavenging. Depletion of
999 oxygen may favor the MeHg formation. However, the multi-causal drivers of Hg
1000 methylation and demethylation rates add complexity to any attempts to predict future
1001 effects. Besides, a reduction in European atmospheric emissions would lead to a decrease
1002 in Hg deposition to the MED, and the short Hg residence time in waters should favor a
1003 rapid decline of Hg concentrations in waters. Climate change may induce in the MED not
1004 only a reduction of primary productivity but changes in phytoplankton community
1005 composition and likely a decrease in cell size, as already observed in different geographic
1006 zones^{243, 244, 245}. Human coastal management may also impact terrestrial inputs, such as
1007 the decrease of phosphorus inputs to the Mediterranean rivers in recent decades inducing
1008 a decrease in plankton size²⁴⁶. An increase in oligotrophy and a decrease in cell size may
1009 thus increase Hg bioconcentration processes at the base of food webs. At higher trophic

1010 levels, an increase in temperature would increase the metabolic demand of organisms¹⁸⁶
1011 and affect their behavior¹⁸⁵, leading to a decrease in their growth rate and size that could
1012 cause an increase of MeHg bioaccumulation and a decrease in its elimination rate¹⁶⁷. A
1013 decrease in organism size generally leads to longer and less efficient food webs, along
1014 which Hg biomagnification would be increased, while the effects of temperature on food
1015 web length are complex and may vary spatially^{192, 247, 248}. Thus, the three Hg transfer
1016 processes in biota, bioconcentration, bioaccumulation, and biomagnification could be
1017 enhanced by different climate change scenarios in the MED¹⁵⁸, but its intensity would
1018 probably be highly spatially heterogeneous. An increase in Hg concentrations in marine
1019 organisms would be problematic for seafood consumers in the MED region.

1020 ***8.2. The unknowns of the Mediterranean Hg cycle and research needs***

1021 Despite the numerous scientific advances described in this review paper, several
1022 uncertainties in the MED Hg distribution, cycling, and budget persist.

- 1023 – Measurements of THg and MeHg in the Southern MED and the Levantine Basin
1024 waters are insufficient for mapping oceanographically consistent distributions of
1025 Hg species in the water column of the EMED.
- 1026 – The revised Hg budget for the MED remains poorly constrained relatively to
1027 several Hg inputs especially because of the almost total absence of spatial and
1028 seasonal data series, including speciation, and fluxes at the air-sea interface,
1029 hydrothermal vents, cold seeps, SGD, and point sources. Monitoring systems for
1030 seasonally quantifying continental inputs have to be implemented.
- 1031 – Notwithstanding a general agreement for a net Hg evasion flux ($\sim 30 \text{ Mg y}^{-1}$) to
1032 the atmosphere, taking into account the photolytic reduction of Hg^{II} compounds in
1033 the atmosphere could modify this figure. Gas-phase reduction of Hg^{II} would
1034 reduce dry and wet deposition to the MED, however by how much, requires
1035 further modeling studies to be performed. In addition, at-sea monitoring of
1036 seasonal and spatial variability (coastal upwelling) of Hg deposition and evasion
1037 is needed to explore to what extent atmospheric deposition is the primary factor
1038 controlling evasion of Hg^0 to the atmosphere. Such data will provide the basis for
1039 models and for validating them.
- 1040 – The transport of particulate Hg inputs from terrigenous origin to the open sea
1041 through canyons is not adequately quantified. For example, which part of riverine
1042 Hg inputs (associated with particulate material) remains in the margin sediments,

- 1043 which part reaches the abyssal sediments *via* canyons, which part is released in
1044 the water column, and which part may become available to benthic food webs?
- 1045 – Some aspects of Hg speciation in waters are still questionable. For example,
1046 published observations on MMHg/DMHg ratios diverge widely in space and time
1047 and show little coherence or rationale. The ratio between the two methylated
1048 forms has consequences for MeHg fate and distribution between the atmosphere,
1049 water, and biota.
- 1050 – Further work is also needed to elucidate Hg methylation mechanisms. The
1051 biogeochemical factors which promote net Hg methylation are still being
1052 identified. The importance of the nutrient status (and associated plankton
1053 communities) appears to be a determining criterion. Indeed, we know that the
1054 oligotrophic EMED waters are less loaded with MeHg than the WMED. To what
1055 extent is the heterotrophic activity responsible for Hg methylation, especially in
1056 phosphate-limited environments? Is there a place for abiotic methylation?
- 1057 – The main challenge to advancing the understanding of Hg transfer in MED marine
1058 food webs resides in the clarification, and quantification, of bioconcentration
1059 processes at the base of the food chain, by far the largest “quantum” leap in Hg
1060 concentration in biota. This challenge comes with several questions:
- 1061 ○ What are the relative roles of food web length, plankton size and nature,
1062 and detritus in the transfer efficiency of MeHg?
 - 1063 ○ How would differences in biomass of the various groups of viruses,
1064 bacteria, autotrophic and heterotrophic pico, and nanoplankton cells affect
1065 Hg bioaccumulation in zooplankton consumers?
 - 1066 ○ Could the oligotrophic conditions modify the importance of the microbial
1067 loop as well as the role played by mixotrophic organisms in the trophic
1068 transfer of Hg?
 - 1069 ○ Rather few data are available on Hg and MeHg concentrations in the
1070 benthic invertebrates which constitute important prey sources for higher
1071 trophic level consumers. Are there different processes involved in Hg
1072 transfer and biomagnification in pelagic and benthic-dominated food
1073 webs?

1074 To sum up, a strategy for building a comprehensive understanding of the Hg cycle
1075 in the MED, allowing future assessment of global change impacts in conjunction with

1076 the Minamata Convention Hg policy, should be based on long-term time-series
1077 observations, the use of new markers (e.g., Hg isotopes), and high-resolution Earth
1078 System Models dedicated to the MED area. Understanding, representing, and
1079 quantifying the interlinked processes involved in the Hg cycle, from earth system
1080 physics to microbial transformations, is far from trivial. Although the levels of
1081 uncertainty associated with individual processes are still high, models can be useful in
1082 dealing with such uncertainty through scenario analyses^{45, 78, 224}. Coupled physical-
1083 biogeochemical numerical models can help in investigating the impacts of climate
1084 change on marine ecosystems focusing on Hg biogeochemistry and its interconnections
1085 with transport and transformation phenomena^{33, 218, 219, 224} allowing different hypotheses
1086 and scenarios to be tested. Future efforts should be made in coupling Hg models into
1087 integrated regional and/or earth system models, able to describe Hg cycling through the
1088 ocean, atmosphere, and biosphere, and to properly consider contamination hot spots, and
1089 impacts on regions of particular interest, such as coastal areas^{249, 250}. Such a challenge
1090 calls for a combination of modeling refinement, from the use of variable spatial mesh
1091 and/or downscaling, to a better parameterization of transport and transformation
1092 processes, aerosols, and Hg bioaccumulation and magnification in terrestrial and marine
1093 ecosystems. Such integrated modeling is the ultimate step in building realistic scenarios
1094 of Hg cycle evolution in the Mediterranean environment. New spatial and dynamic end-
1095 to-end ecosystem modeling which relates trophic transfer and Hg and MeHg transfer,
1096 based on field data should be developed to relate observations of physical and
1097 biogeochemical processes to marine resource exploitation and consumption. Such
1098 integrated models are required to test scenarios and to be used as mitigation and
1099 management tools.

1100

1101 **ACRONYMS**

1102 AOU: Apparent oxygen utilization
1103 AW: Atlantic Water
1104 DGM: Dissolved gaseous mercury
1105 DMHg: Dimethyl mercury
1106 DMW: Deep Mediterranean Water
1107 EIW: Eastern Intermediate Water
1108 EMED: Eastern Mediterranean
1109 EU: European Union
1110 GEM: Gaseous elemental mercury
1111 GMA: Global mercury assessment

1112 GMOS: Global mercury observation system
1113 GOM: Gaseous oxidized mercury
1114 Hg: Mercury
1115 INMA: Environment and Childhood Project (ISGlobal, Spain)
1116 MED: Mediterranean
1117 MeHg: Methylated mercury (MMHg+DMHg)
1118 MMHg: Monomethyl mercury
1119 NWMED: Northwestern Mediterranean
1120 OM: Organic matter
1121 OMZ: Oxygen minimum zone
1122 PHIME: Public Health Impact of Long-Term, Low-level Mixed Element Exposure in
1123 Susceptible Population Strata (USA Department of Agriculture)
1124 SGD: Submarine groundwater discharge
1125 TDW: Tyrrhenian Deep Water
1126 TMF: Trophic magnification factor
1127 TMS: Trophic magnification slope
1128 UNEP: United Nations Environment Programme
1129 WHO: World Health Organization
1130 WMDW: Western Mediterranean deep water
1131 WMED: Western Mediterranean

1132

1133 **Supporting Information**

1134 SI.1. Summary of the biogeochemical Hg cycle; SI.2. Calculation of the gas transfer
1135 velocities at the Mediterranean air-sea interface; SI.3. Summary statistics on total Hg
1136 concentrations in the western Mediterranean waters; SI.4. Methylated mercury in
1137 various oceanic basins; SI.5. Biological methylation and demethylation mechanisms;
1138 SI.6. Calculations of total and methylated Hg masses in Mediterranean marine biota;
1139 SI.7. Total and methylated Hg content in Mediterranean biota; SI.8. Mercury levels in
1140 exposure biomarkers in humans in the Mediterranean countries.

1141

1142 **ACKNOWLEDGEMENTS**

1143 This research has been funded by the Global Mercury Observation System (GMOS, N-
1144 265113 European Commission project), and the European Research Council (ERC-
1145 2010-StG-20091028). The authors acknowledge the financial support from the project
1146 Integrated Global Observing Systems for Persistent Pollutants (IGOSP) funded by the
1147 European Commission in the framework “The European network for observing our
1148 changing planet (ERA-PLANET)” program, Grant Agreement: 689443. This work also
1149 received support from the MISTRALS transversal action on pollutants and contaminants
1150 (INSU-CNRS). Thanks are due to M. Coquery for providing unpublished MeHg values

1151 from deep Mediterranean sediments, M. Petrova for THg concentrations in SGDs of
1152 Marseille region (France), and I. Taupier-Letage for her guidance in preparing figure 1.

References

- ¹ *UN-Environment. Global Mercury Assessment 2018*. United Nation Environmental Programme, Chemicals and Health Branch, Programme Chemicals and Health Branch Geneva Switzerland. 2019; www.unenvironment.org/resources/publication/global-mercury-assessment-2018.
- ² Boening, D. W. Ecological effects, transport, and fate of mercury: a general review. *Chemosphere* **2010**, *40*, 1335-1351 ; DOI 10.1016/S0045-6535(99)00283-0.
- ³ Chen, C. 2012. Methylmercury Effects and Exposures: Who Is a Risk? *Environ. Health Perspect.* **2012**, *120*, A224-225 ; DOI 10.1289/ehp.1205357.
- ⁴ Eagles-Smith, C. A.; Silbergeld, E. K.; Basu, N.; Bustamante, P.; Diaz-Barriga, F.; Hopkins, W. A.; Kidd, K. A.; Nyland, J. F. Modulators of mercury risk to wildlife and humans in the context of rapid global change. *Ambio* **2018**, *47*, 170–197 ; DOI:10.1007/s13280-017-1011-x.
- ⁵ Clarkson, T. W. The Three Modern Faces of Mercury. *Environ. Health Perspect.* **2002**, *110*, 11-23 ; DOI 10.1289/ehp.02110s111.
- ⁶ *National Research Council, USA. Toxicological Effects of Methylmercury*. National Academy Press, Washington, DC 20055, USA. **2000**. ISBN-10: 0-309-07140-2. <https://www.nap.edu/read/9899.html>.
- ⁷ Roman, H. A.; Walsh, T. L.; Coull, B. A.; Dewailly, É.; Guallar, E.; Hattis, D.; Mariën, K.; Schwartz, J.; Stern, A. H.; Virtanen, J. K.; Rice, G. Evaluation of the Cardiovascular Effects of Methylmercury Exposures: Current Evidence Supports Development of a Dose–Response Function for Regulatory Benefits Analysis. *Environ. Health Persp.* **2011**, *19*, 5 ; DOI 10.1289/ehp.1003012.
- ⁸ Bradley, M. A.; Barst, B. D.; Basu, N. A Review of Mercury Bioavailability in Humans and Fish. *Int. J. Environ. Res. Public Health* **2017**, *14*, 169-189 ; DOI 10.3390/ijerph14020169.
- ⁹ Debes, F.; Budtz-Jorgensen, E.; Weihe, P.; White, R. F.; Grandjean, P. 2006. Impact of prenatal methylmercury exposure on neurobehavioral functions at age of 14 years. *Neurotoxicol. Teratol.* **2006**, *28*, 536-547 ; DOI 10.1016/j.ntt.2006.02.005.
- ¹⁰ Petrova, M. V.; Ourgaud, M.; Boavida, J. R. H.; Dufour, A.; Tesán Onrubia, J. A.; Lozingot, A.; Heimbürger-Boavida, L.-E. 2020. Human mercury exposure levels and fish consumption at the French Riviera. *Chemosphere* **2020**, *258*, 127232 ; DOI 10.1016/j.chemosphere.2020.127232.
- ¹¹ Driscoll, C. T.; Mason, R. P.; Chang, H. M.; Jacobs, D. J.; Pirrone, N. Mercury as a Global Pollutant: Sources, Pathways an Effects. *Environ. Sci. Technol.* **2013**, *47*, 4967-4983 ; DOI 10.1021/es305071v.
- ¹² Lamborg, C.; Bowman, K.; Hammerschmidt, C.; Gilmour, C.; Munson, K.; Selin, N.; Tseng, C.-M. Mercury in the Anthropocene Ocean. *Oceanography* **2014**, *27*, 76–87 ; DOI 10.5670/oceanog.2014.11.
- ¹³ Outridge, P. M.; Mason, R. P.; Wang, F.; Guerrero, S.; Heimbürger-Boavida, L.-E. Updated Global and Oceanic Mercury Budgets for the United Nations Global Mercury Assessment 2018. *Environ. Sci. Technol.* **2018**, *52*, 12968–12977 ; DOI 10.1021/acs.est.8b04542.
- ¹⁴ Martínez-Cortizas, A.; Pontevedra-Pombal, X.; García-Rodeja, E.; Nóvoa-Muñoz, J. C.; Shotyk, W. Mercury in a Spanish Peat Bog: Archive of Climate Change and Atmospheric Metal Deposition. *Science* **1999**, *287*, 939-941 ; DOI 10.1126/science.284.5416.939.
- ¹⁵ Streets, D. G., Horowitz, H. M.; Lu, Z.; Levin, L.; Thackray, C. P.; Sunderland, E. M. Global and regional trends in mercury emissions and concentrations, 2010–2015. *Atmos. Environ.* **2019**, *201*, 417-427 ; DOI 10.1016/j.atmosenv.2018.12.031.
- ¹⁶ Streets, D. G., Horowitz, H. M.; Lu, Z.; Levin, L.; Thackray, C. P.; Sunderland, E. M. Five hundred years of anthropogenic mercury: spatial and temporal release profiles. *Environ. Res. Lett.* **2019**, *14*(8), 084004 ; DOI 10.1088/1748-9326/ab281f.
- ¹⁷ Thibaud, Y. Teneur en mercure dans quelques poissons de consommation courante. *Sciences et Pêches, Bull. Inst. Pêches marit.* **1971**, XXII-XIII 79, pp. 10.

-
- ¹⁸ Bernhard, M.; Renzoni, A. Mercury concentration in Mediterranean marine organisms and their environment: Natural or anthropogenic origin. *Thalassia Jugoslavica* **1977**, *3*, 265–300.
- ¹⁹ Renzoni, A.; Bernard, M.; Sara, R.; Stoeppler, M. Comparison between the Hg body burden of *Thynnus thynnus* from the Mediterranean and the Atlantic. IVème Journées d'Etude de la Pollution, Antalya, CIESM, Monaco, 255, **1979**.
- ²⁰ Aston, S. R.; Fowler S. W. Mercury in the open Mediterranean: evidence of contamination. *Sci. Total Environ.* **1985**, *43*, 13-18 ; DOI 10.1016/0048-9697(85)90028-2.
- ²¹ Cossa, D.; Harmelin-Vivien, M.; Mellon-Duval, C.; Loizeau, V.; Averty, B.; Crochet, S.; Chou, L.; Cadiou, J.-F. Influences of Bioavailability, Trophic Position, and Growth on Methylmercury in Hakes (*Merluccius merluccius*) from Northwestern Mediterranean and Northeastern Atlantic. *Environ. Sci. Technol.* **2012**, *46*, 4885-4893 ; DOI 10.1021/es204269w.
- ²² Tseng, C. M.; Ang, S. J.; Chen, Y. S.; Shiao, J. C.; Lamborg, C. H.; He, X.; Reinfelder, J. R. Bluefin tuna reveal global patterns of mercury pollution and bioavailability in the world's oceans. *Pro. Natl. Acad. Sci. U.S.A.*, **2021**, *118*, 1-6 ; DOI 10.1073/pnas.2111205118.
- ²³ Albertos, S.; Berenguer, N. I.; Sánchez-Virosta, P.; Gómez-Ramírez, P.; Jiménez, P.; Torres-Chaparro, M. Y.; Valverde, I.; Navas, I.; María-Mojica, P.; García-Fernández, A. J.; Espín, S. Mercury Exposure in Birds Linked to Marine Ecosystems in the Western Mediterranean. *Arch. Environ. Contam. Toxicol.* **2020**, *79*, 435–453 ; DOI 10.1007/s00244-020-00768-1.
- ²⁴ Gustin, M. S.; Bowman, K.; Branfireun, B.; Chetelat, J.; Eckley, C. S.; Hammerschmidt, C. R.; Lamborg, C.; Lyman, S.; Martinez-Cortizas, A.; Sommar, J.; Tsui, M. T.-K.; Zhang, T. Mercury biogeochemical cycling: A synthesis of recent scientific advances. *Sci. Total Environ.* **2020**, *737*, 139619 ; DOI 10.1016/j.scitotenv.2020.139619.
- ²⁵ AMAP/UN Environment. *Technical Background Report for the Global Mercury Assessment 2018*. Arctic Monitoring and Assessment Programme, Oslo, Norway/UN Environment Programme, Chemicals and Health Branch, Geneva, Switzerland. viii + 426 pp including E-Annexes. **2019**. <https://www.amap.no/documents/doc/technical-background-report-for-the-global-mercury-assessment-2018/1815>.
- ²⁶ Crise, A.; Allen, J. I.; Baretta, J.; Crispi, G.; Mosetti, R.; Solidoro, C. The Mediterranean pelagic ecosystem response to physical forcing. *Progr. Oceanogr.* **1999**, *44*, 219-243 ; DOI 10.1016/S0079-6611(99)00027-0.
- ²⁷ Millot, C.; Taupier-Letage, I. Circulation in the Mediterranean. In *The Mediterranean Sea*; Saliot, A. Ed.; Hdb. Env. Chem. Vol. 5, Part K, 29–66. Springer-Verlag Berlin Heidelberg 2005; pp 414; DOI 10.1007/b107143.
- ²⁸ Richon, C.; Dutay, J.-C.; Bopp, L.; Le Vu, B.; Orr, J. C.; Somot, S.; Dulac, F. Biogeochemical response of the Mediterranean Sea to the transient SRES-A2 climate change scenario. *Biogeosciences* **2019**, *16*, 135-165 ; DOI 10.5194/bg-16-135-2019.
- ²⁹ Durrieu de Madron, X.; Guieu, C.; Sempéré, R.; Conan, P.; Cossa, D.; D'Ortenzio, F.; Estournel, C.; Gazeau, F.; Rabouille, C.; Stemmann, L.; Bonnet, S.; Diaz, F.; Koubbi, P.; Radakovitch, O.; Babin, M.; Baklouti, M.; Bancon-Montigny, C.; Belviso, S.; Bensoussan, N.; Bonsang, B.; Bouloubassi, I.; Brunet, C.; Cadiou, J.-F.; Carlotti, F.; Chami, M.; Charmasson, S.; Charrière, B.; Dachs, J.; Doxaran, D.; Dutay, J.-C.; Elbaz-Poulichet, F.; Eléaume, M.; Eyrolles, F.; Fernandez, C.; Fowler, S.; Francour, P.; Gaertner, J. C.; Galzin, R.; Gasparini, S.; Ghiglione, J.-F.; Gonzalez, J.-L.; Goyet, C.; Guidi, L.; Guizien, K.; Heimbürger, L.-E.; Jacquet, S. H. M.; Jeffrey, W. H.; Joux, F.; Le Hir, P.; Leblanc, K.; Lefèvre, D.; Lejeune, C.; Lemé, R.; Loÿe-Pilot, M.-D.; Mallet, M.; Méjanelle, L.; Mélin, F.; Mellon, C.; Mérigot, B.; Merle, P.-L.; Migon, C.; Miller, W. L.; Mortier, L.; Mostajir, B.; Mousseau, L.; Moutin, T.; Para, J.; Pérez, T.; Petrenko, A.; Poggiale, J.-C.; Prieur, L.; Pujo-Pay, M.; Pulido-Villena, Raimbault, P.; Rees, A. P.; Ridame, C.; Rontani, J.-F.; Ruiz Pino, D.; Sicre, M. A.; Taillandier, V.; Tamburini, C.; Tanaka, T.; Taupier-Letage, I.; Tedetti, M.; Testor, P.; Thébault, H.; Thouvenin, B.; Touratier, F.; Tronczynski, J.; Ulses, C.; Van Wambeke, F.; Vantrepotte, V.; Vaz, S.; Verney, R. Marine ecosystems' responses to climatic and anthropogenic forcings in the Mediterranean. *Prog. Oceanogr.* **2011**, *91*, 97–166 ; DOI 10.1016/j.pcean.2011.02.003.
- ³⁰ Horvat, M.; Covelli, S.; Faganelli, J.; Logar, M.; Mandic, V.; Rajar, R.; Sirca, A.; Zagar, D. Mercury in contaminated coastal environments; a case study: the Gulf of Trieste. *Sci. Total Environ.* **1999**, *237-238*, 43-56 ; DOI 10.1016/S0048-9697(99)00123-0.

-
- ³¹ Covelli, S.; Langone, L.; Acquavita, A.; Piani, R.; Andrea, E. Historical flux of mercury associated with mining and industrial sources in the Marano and Grado Lagoon (northern Adriatic Sea). *Estuar. Coast Shelf Sci.* **2012**, *113*, 7–9.
- ³² Canu, D. M.; Rosati, G.; Solidoro, C.; Heimbürger, L. E.; Acquavita, A. A comprehensive assessment of the mercury budget in the Marano–Grado Lagoon (Adriatic Sea) using a combined observational modeling approach. *Mar. Chem.* **2015**, *177*, 742–752 ; DOI 10.1016/j.marchem.2015.10.013.
- ³³ Rosati, G.; Solidoro, C.; Canu, D. Mercury dynamics in a changing coastal area over industrial and postindustrial phases: Lessons from the Venice Lagoon. *Sci. Total Environ.* **2020**, *743*, 1–15 ; DOI 10.1016/j.scitotenv.2020.140586.
- ³⁴ Tessier, E.; Garnier, C.; Mullot, J.-U.; Lenoble, V.; Arnaud, M.; Raynaud, M.; Mounier, S. Study of the spatial and historical distribution of sediment inorganic contamination in the Toulon bay (France). *Mar. Pollut. Bull.* **2011**, *62*, 2075–2086 ; DOI 10.1016/j.marpolbul.2011.07.022.
- ³⁵ German, C. R. C.; Casciotti, K. A.; Dutay, J.-C.; Heimbürger, L. E.; Jenkins, W. J.; Measures, C. I.; Mills, R. A.; Obata, H.; Schlitzer, R.; Tagliabue, A.; Turner, D. R.; Whitby, H. Hydrothermal impacts on trace element and isotope ocean biogeochemistry. *Phil. Trans. R. Soc., A Math. Phys. Eng. Sci.* **2016**, *374*, 20160035 ; DOI 10.1098/rsta.2016.0035.
- ³⁶ Bagnato, E.; Oliveri, E.; Acquavita, A.; Covelli, S.; Petranich, E.; Barra, M.; Italiano, F.; Parello, F.; Sprovieri, M. Hydrochemical mercury distribution and air-sea exchange over the submarine hydrothermal vents off-shore Panarea Island (Aeolian arc, Tyrrhenian Sea). *Mar. Chem.* **2017**, *194*, 63–78 ; DOI 10.1016/j.marchem.2017.04.003.
- ³⁷ Ferrara, R.; Mazzolai, B.; Lanzillotta, E.; Nucaro, E.; Pirrone, N. Volcanoes as emission sources of atmospheric mercury in the Mediterranean basin. *Sci. Total Environ.* **2000**, *259*, 115–121 ; DOI 10.1016/S0048-9697(00)00558-1.
- ³⁸ Edwards, B. A.; Kushner, D. S.; Outridge, P. M.; Wang, F. Fifty years of volcanic mercury emission research: Knowledge gaps and future directions. *Sci. Total Environ.* **2020**, *757*, 143800 ; DOI 10.1016/j.scitotenv.2020.143900.
- ³⁹ Cossa, D.; Martin, J.-M.; Takayanagi, K.; Sanjuan, J. The Distribution and Cycling of Mercury in the Western Mediterranean. *Deep Sea Res. II* **1997**, *44*, 721–740 ; DOI 10.1016/S0967-0645(96)00097-5.
- ⁴⁰ Rajar, R.; Četina, M.; Horvat, M.; Žagar, D. Mass balance of mercury in the Mediterranean Sea. *Mar. Chem.* **2007**, *107*, 89–102 ; DOI 10.1016/j.marchem.2006.10.001.
- ⁴¹ Žagar, D.; Sirk, N.; Četina, M.; Horvat, M.; Kotnik, J.; Ogrinc, N.; Hedgecock, I. M.; Cinnirella, S.; de Simone, F.; Gencarelli, C. N.; Pirrone, N. Mercury in the Mediterranean. Part 2: processes and mass balance. *Environ. Sci. Pollut. Res.* **2014**, *21*, 4081–4094 ; DOI 10.1007/s11356-013-2055-5.
- ⁴² Ogrinc, N.; Kotnik, J.; Fajon, V.; Monperrus, M.; Kocman, D.; Vidimova, K.; Amouroux, D.; Žižek, S.; Horvat, M. Distribution of Mercury and Methylmercury in Sediments of the Mediterranean Sea. *Mar. Chem.* **2007**, *107*, 31–48 ; DOI 10.1016/j.marchem.2007.01.019.
- ⁴³ Cossa, D.; Durrieu de Madron, X.; Schäfer, J.; Lancelot, L.; Guédron, S.; Buscail, R.; Thomas, B.; Naudin, J.-J. The open sea as the main source of methylmercury in the water column of the Gulf of Lions (Northwestern Mediterranean margin). *Geochim. Cosmochim. Acta* **2017**, *199*, 212–231 ; DOI 10.1016/j.gca.2016.11.037.
- ⁴⁴ Monperrus, M.; Tessier, E.; Amouroux, D.; Leynaert, A.; Huonnic, P.; Donard, O. F. X. Mercury methylation, demethylation and reduction rates in coastal and marine surface waters of the Mediterranean Sea. *Mar. Chem.* **2007**, *107*, 49–63. DOI 10.1016/j.marchem.2007.01.018.
- ⁴⁵ Rosati, G.; Heimbürger, L. E.; Melaku Canu, D.; Lagane, C.; Laffont, L.; Rijkenberg, M. J. A.; Gerringa, L. J. A.; Solidoro, C.; Gencarelli, C. N.; Hedgecock, I. M.; de Baar, H. J. W.; Sonke, J. E. Mercury in the Black Sea: New insights from measurements and numerical modeling. *Global Biogeochem. Cy.* **2018**, *32* ; DOI 10.1002/2017GB005700.
- ⁴⁶ Cossa, D.; Knoery, J.; Boye, M.; Maruszczak, N.; Thomas, B.; Courau, P.; Sprovieri, F. Oceanic mercury concentrations on both sides of the Strait of Gibraltar decreased between 1989 and 2012. *Anthropocene* **2019**, *29*, 100230. Doi.org/10.1016/j.ancene.2019.100230.

-
- ⁴⁷ Fenoglio-Marc, L.; Mariotti, A.; Sannino, G.; Meyssignac, B.; Carillo, A.; Struglia, M. V.; Rixen, M. Decadal variability of net water flux at the Mediterranean Sea Gibraltar Strait. *Glob. Planet. Change* **2013**, *100*, 1-10 ; DOI 10.1016/j.gloplacha.2012.08.007.
- ⁴⁸ Chouvelon, T.; Cresson, P.; Bouchoucha, M.; Brach-Papa, C.; Bustamante, P.; Crochet, S.; Fabri, M.-C.; Marco-Miralles, F.; Thomas, B.; Knoery, J. Oligotrophy as a major driver of Hg bioaccumulation in marine medium- to high-trophic level consumers: an ecosystem-comparative study. *Environ. Pollut.* **2018**, *233*, 844-854 ; DOI j.envpol.2017.11.015.
- ⁴⁹ Wang, F.; Outridge, P. M.; Feng, X.; Meng, B.; Heimbürger-Boavida, L.-E.; Mason R. P. How closely do mercury trends in fish and other aquatic wildlife track those in the atmosphere? - Implications for evaluating the effectiveness of the Minamata Convention. *Sci. Total Environ.* **2019**, *674*, 58–70 ; DOI 10.1016/j.scitotenv.2019.04.101.
- ⁵⁰ Pirrone, N.; Costa, P.; Pacyna, J. M.; Ferrara, R. Mercury emissions to the atmosphere from natural and anthropogenic sources in the Mediterranean region. *Atmos. Environ.* **2001**, *35*(17), 2997-30006 ; DOI 10.1016/S1352-2310(01)00103-0.
- ⁵¹ Cinnirella, S.; Pirrone, N.; Allegrini, A.; Guglietta, D. Modeling mercury emissions from forest fires in the Mediterranean region. *Environ. Fluid. Mech.* **2008**, *8*, 129–145 ; DOI 10.1007/s10652-007-90.
- ⁵² Sprovieri, F.; Pirrone, N.; Gårdfeldt, K.; Sommar, J. Atmospheric Mercury Speciation in the Marine Boundary Layer along 6000 km Cruise path over the Mediterranean Sea. *Atmos. Environ.* **2003**, *37/S1*, 63-71 ; DOI 10.1016/S1352-2310(03)00237-1.
- ⁵³ Sprovieri, F.; Hedgecock, I. M.; Pirrone, N. An investigation of the origins of reactive gaseous mercury in the Mediterranean marine boundary layer. *Atmos. Chem. Phys.* **2010**, *10*, 3985-3997 ; DOI:10.5194/acp-10-3985-2010.
- ⁵⁴ Hedgecock, I. M., Pirrone, N., Sprovieri, F., Pesenti, E. 2003. Reactive Gaseous Mercury in the Marine Boundary Layer: Modeling and Experimental Evidence of its Formation in the Mediterranean. *Atmos. Environ.* **2003**, *37/S1*, 41-49 ; DOI 10.1016/S1352-2310(03)00236-X.
- ⁵⁵ Hedgecock, I. M.; Pirrone, N. Chasing Quicksilver: Modeling the Atmospheric Lifetime of Hg⁰(g) in the Marine Boundary Layer at Various Latitudes. *Environ. Sci. Technol.* **2004**, *38*, 69–76 ; DOI.org/10.1021/es034623z.
- ⁵⁶ Wängberg, I.; Munthe, J.; Amouroux, D.; Andersson, M. E.; Fajon, V.; Ferrara, R.; Gårdfeldt, K.; Horvat, M.; Mamane, Y.; Melamed, E.; Monperrus, M.; Ogrinc, N.; Yossef, O.; Pirrone, N.; Sommar, J.; Sprovieri, F. 2008. Atmospheric mercury at Mediterranean coastal stations. *Environ. Fluid Mech.* **2008**, *8*(2), 101-116 ; DOI 10.1007/s10652-007-9047-2.
- ⁵⁷ Gårdfeldt, K.; Sommar, J.; Ferrara, R.; Ceccarini, C.; Lanzillotta, E.; Munthe, J.; Wängberg, I.; Lindqvist, O.; Pirrone, N.; Sprovieri, F.; Pesenti, E.; Strömberg, D. Evasion of mercury from coastal and open waters of the Atlantic Ocean and the Mediterranean Sea. *Atmos. Environ.* **2003**, *37*, 73 - 84 ; DOI 10.1016/S1352-2310(03)00238-3.
- ⁵⁸ Andersson, M. E.; Gårdfeldt, K.; Wängberg, I.; Sprovieri, F.; Pirrone, N.; Lindqvist, O. Seasonal and daily variation of mercury evasion at coastal and off shore sites from the Mediterranean Sea. *Mar. Chem.* **2007**, *104*, 214 - 226 ; DOI 10.1016/j.marchem.2006.11.003.
- ⁵⁹ Fantozzi, L.; Manca, G.; Ammoscato, I.; Pirrone, N.; Sprovieri, F. The cycling and sea–air exchange of mercury in the waters of the Eastern Mediterranean during the 2010 MED-OCEANOR cruise campaign. *Sci. Total Environ.* **2013**, *448*(15), 151-162 ; DOI 10.1016/j.scitotenv.2012.09.062.
- ⁶⁰ Nerentorp Mastro Monaco, M. G.; Gårdfeldt, K.; Wängberg, I. Seasonal and spatial evasion of mercury from the western Mediterranean Sea. *Mar. Chem.* **2017**, *193*, 34–43 ; DOI 10.1016/j.marchem.2017.02.003, 2017b.
- ⁶¹ Liss, P. S.; Slater, P. G. Flux of Gases across the Air-Sea Interface. *Nature* **1974**, *247*(5438), 181-184 ; DOI 10.1038/247181a0.
- ⁶² Liss, P. S.; Merlivat, L. Air-Sea Gas Exchange Rates: Introduction and Synthesis. In *The Role of Air-Sea Exchange in Geochemical Cycling*; Buat-Ménard P. Ed.; NATO ASI Series (Series C: Mathematical and Physical Sciences, Vol 185). Springer, Dordrecht 1986; pp 549 ; DOI 10.1007/978-94-009-4738-2-5.

-
- ⁶³ Wanninkhof, R. Relationship between wind speed and gas exchange over the ocean. *J. Geophys. Res.* **1992**, *97*(C5), 7373-7382 ; DOI 10.1029/92JC00188.
- ⁶⁴ Wanninkhof, R.; McGillis, W. R. A cubic relationship between air-sea CO₂ exchange and wind speed. *Geophys. Res. Letters* **1999**, *26*(13), 1889-1892 ; DOI 10.1029/1999GL900363.
- ⁶⁵ Nightingale, P. D.; Malin, G.; Law, C. S.; Watson, A. J.; Liss, P. S.; Liddicoat, M. I.; Boutin, J.; Upstill-Goddard, R. C. In situ evaluation of air-sea gas exchange parameterizations using novel conservative and volatile tracers. *Global Biogeochem. Cy.* **2000**, *14*(1), 373-387 ; DOI 10.1029/1999GB900091.
- ⁶⁶ McGillis, W. R.; Edson, J. B.; Hare, J. E.; Fairall, C. W. Direct covariance air-sea CO₂ fluxes. *J. Geophys. Res. Oceans* **2001**, *106*(C8), 16729-16745 ; DOI 10.1029/2000JC000506.
- ⁶⁷ Johnson, M. T. A numerical scheme to calculate temperature and salinity dependent air-water transfer velocities for any gas. *Ocean Sci.* **2010**, *6*(4), 913-932 ; DOI 10.5194/os-6-913-2010.
- ⁶⁸ Zhang, L.; Zhou, P.; Cao, S.; Zhao, Y. Atmospheric mercury deposition over the land surfaces and the associated uncertainties in observations and simulations: a critical review. *Atmos. Chem. Phys.* **2019**, *19*, 15587-15608 ; DOI 10.5194/acp-19-15587-2019
- ⁶⁹ Tomazic, Š.; Ličer, M.; Žagar, D. Numerical modelling of mercury evasion in a two-layered Adriatic Sea using a coupled atmosphere-ocean model ocean model. *Mar. Pollut. Bull.* **2018**, *135*, 1164-1173 ; DOI 10.1016/j.marpolbul.2018.08.064
- ⁷⁰ Sharif, A.; Tessier, E.; Bouchet, S.; Monperrus, M.; Pinaly, H.; Amouroux, D. Comparison of Different Air-Water Gas Exchange Models to Determine Gaseous Mercury Evasion from Different European Coastal Lagoons and Estuaries. *Water Air Soil Pollut.* **2013**, *224*(7), 1606 ; DOI 10.1007/s11270-013-1606-1.
- ⁷¹ Abril, G.; Commarieu, M.-V.; Sottolichio, A.; Bretel, P.; Guérin, F. Turbidity limits gas exchange in a large macrotidal estuary. *Estuar. Coast. Shelf Sci.* **2009**, *83*, 342-348 ; DOI 10.1016/j.ecss.2009.13.006.
- ⁷² Bagnato, E.; Sproveri, M.; Barra, M.; Bitetto, M.; Bonsignore, M.; Calabrese, S.; Stefano, V. D.; Oliveri, E.; Parello, F.; Mazzola, S. The sea-air exchange of mercury (Hg) in the marine boundary layer of the Augusta basin (southern Italy): Concentrations and evasion flux. *Chemosphere* **2013**, *93*(9), 2024 - 2032 ; DOI 10.1016/j.chemosphere.2013.07.025.
- ⁷³ Floreani, F.; Acquavita, A.; Petranich, E.; Covelli, S. Diurnal fluxes of gaseous elemental mercury from the water-air interface in coastal environments of the northern Adriatic Sea. *Sci. Total Environ.* **2019**, *668*, 925 - 935 ; DOI 10.1016/j.scitotenv.2019.03.012.
- ⁷⁴ Sommar, J.; Osterwalder, S.; Zhu, W. Recent advances in understanding and measurement of Hg in the environment: Surface-atmosphere exchange of gaseous elemental mercury (Hg⁰). *Sci. Total Environ.* **2020**, *721*, 137648 ; DOI 10.1016/j.scitotenv.2020.137648.
- ⁷⁵ Cossa, D.; Coquery, M. The Mediterranean mercury anomaly, a geochemical or a biological issue. In *The Mediterranean Sea*; Saliot, A. Ed.; Hdb. Env. Chem. Vol. 5, Part K, 177-208. Springer-Verlag Berlin Heidelberg 2005; pp 414 ; DOI:10.1007/b107147.
- ⁷⁶ Sprovieri, F.; Pirrone, N.; Bencardino, M.; D'Amore, F.; Angot, H.; Barbante, C.; Brunke, E.-G.; Arcega-Cabrera, F.; Cairns, W.; Comero, S.; del Carmen Diéguez, M.; Dommergue, A.; Ebinghaus, R.; Feng, X. B.; Fu, X.; Garcia, P. E.; Gawlik, B. M.; Hageström, U.; Hansson, K.; Horvat, M.; Kotnik, J.; Labuschagne, C.; Magand, O.; Martin, L.; Mashyanov, N.; Mkololo, T.; Munthe, J.; Obolkin, V.; Islas, M. R.; Sena, F.; Somerset, V.; Spandow, P.; Vardèl, M.; Walters, C.; Wängberg, I.; Weigelt, A.; Yang, X.; Zhang, H. Five-year records of mercury wet deposition flux at GMOS sites in the Northern and Southern hemispheres. *Atmos. Chem. Phys.* **2017**, *17*, 2689-2708 ; DOI 10.5194/acp-17-2689-2017.
- ⁷⁷ Gencarelli, C. N.; De Simone, F.; Hedgecock, I. M.; Sprovieri, F.; Pirrone, N. Development and application of a regional-scale atmospheric mercury model based on WRF/Chem: a Mediterranean area investigation. *Environ. Sci. Pollut. Res. Int.* **2014**, *21*(6), 4095-109 ; DOI 10.1007/s11356-013-2162-3.
- ⁷⁸ Gencarelli, C. N.; De Simone, F.; Hedgecock, I. M.; Sprovieri, F.; Yang, X.; Pirrone, N. European and Mediterranean mercury modelling: local and long-range contributions to the deposition flux. *Atmos. Environ.* **2015**, *117*, 162-168, PII: S1352-2310(15)30214-4 ; DOI 10.1016/j.atmosenv.2015.07.015.

-
- ⁷⁹ De Simone, F. D.; Gencarelli, C. N.; Hedgecock, I. M.; Pirrone, N. 2016. A Modeling Comparison of Mercury Deposition from Current Anthropogenic Mercury Emission Inventories. *Environ. Sci. Technol.* **2016**, *50*(10), 5154-5162 ; DOI 10.1021/acs.est.6b00691.
- ⁸⁰ De Simone, F.; D'Amore, F.; Marasco, F.; Carbone, F.; Bencardino, M.; Hedgecock, I.M.; Cinnirella, S.; Sprovieri, F.; Pirrone, N. A Chemical Transport Model Emulator for the Interactive Evaluation of Mercury Emission Reduction Scenarios. *Atmosphere* **2020**, *11*, 878 ; DOI 10.3390/atmos11080878.
- ⁸¹ Horowitz, H. M.; Jacob, D. J.; Zhang, Y.; Dibble, T. S.; Slemr, F.; Amos, H. M.; Schmidt, J. A.; Corbitt, E. S.; Marais, E. A.; Sunderland, E. M. A new mechanism for atmospheric mercury redox chemistry: implications for the global mercury budget. *Atmos. Chem. Phys.* **2017**, *17*(10), 6353-6371 ; DOI 10.5194/acp-17-6353-2017.
- ⁸² Saiz-Lopez, A.; Acuña, A. U.; Trabelsi, T.; Carmona-García, J.; Dávalos, J. Z.; Rivero, D.; Cuevas, C. A.; Kinnison, D. E.; Sitkiewicz, S. P.; Roca-Sanjuán, D.; Francisco, J. S. Gas-Phase Photolysis of Hg(I) Radical Species: A New Atmospheric Mercury Reduction Process. *J. Am. Chem. Soc.* **2019**, *141*, 8698-702 ; DOI 10.1021/jacs.9b02890.
- ⁸³ Yang, X.; Jiskra, M.; Sonke, J.E. Experimental rainwater divalent mercury speciation and photoreduction rates in the presence of halides and organic carbon. *Sci. Total Environ.* **2019**, *697*, 133821 ; DOI 10.1016/j.scitotenv.2019.133821.
- ⁸⁴ Francés-Monerris, A.; Carmona-García, J.; Acuña, A. U.; Dávalos, J. Z.; Cuevas, C. A.; Kinnison, D. E.; Francisco, J. S.; Saiz-Lopez, A.; Roca-Sanjuán, D. Photodissociation Mechanisms of Major Mercury(II) Species in the Atmospheric Chemical Cycle of Mercury. *Angew. Chem. Int. Ed.* **2020**, *59*(19), 7605-7610 ; DOI 10.1002/anie.201915656.
- ⁸⁵ Jiskra, M.; Heimbürger-Boavida, L. E.; Desgranges, M. M.; Petrova, M. V.; Dufour, A.; Ferreira-Araujo, B.; Masbou, J.; Chmeleff, J.; Thyssen, M.; Point, D.; Sonke, J. E. Mercury stable isotopes constrain atmospheric sources to the ocean. *Nature* **2021**, *597*, 678–682 ; DOI 10.1038/s41586-021-03859-8.
- ⁸⁶ Cossa, D.; Durrieu de Madron, X.; Schäfer, J.; Guédron, S.; Maruszczak, N.; Castelle, S.; Naudin, J.-J. Sources and exchanges of mercury in the waters of the Northwestern Mediterranean margin. *Progr. Oceanogr.* **2018**, *163*, 172-183 ; DOI 10.1016/j.pocean.2017.05.002.
- ⁸⁷ Tagliabu, A. *Elemental Distribution: Overview*; Encyclopedia of Ocean Sciences, 3rd edition; 2018 ; DOI 10.1016/B978-0-12-409548-9.10774-2.
- ⁸⁸ Kotnik, J.; Horvat, M.; Ogrinc, N.; Fajon, V.; Žagar, D.; Cossa, D.; Sprovieri, F.; Pirrone, N. Mercury speciation in the Adriatic Sea. *Mar. Pollut. Bull.* **2015**, *96*, 136–148 ; DOI 10.1016/j.marpolbul.2015.05.037.
- ⁸⁹ Heimbürger-Boavida, L. E. Mediterranean Institute of Oceanography, Université Aix-Marseille, France, unpublished results from PEACETIME cruise.
- ⁹⁰ Knoery, J. Ifremer, Centre Atlantique, France. Unpublished results from FENICE-GMOS cruise.
- ⁹¹ Heimbürger, L.-E.; D. Cossa, D.; Marty, J.-C.; Migon, C.; Averty, B.; Dufour, A.; Ras, J. 2010. Methyl mercury distributions in relation to the presence of nano and picophytoplankton in an oceanic water column (Ligurian Sea, North-western Mediterranean). *Geochim. Cosmochim. Acta* **2010**, *74*, 5549-4459 ; DOI.org:10.1016/j.gca.2010.06.036.
- ⁹² Sunderland, E. M.; Krabbenhoft, D. P.; Moreau, J. W.; Strobe, S. A.; Landing, W. M. Mercury sources, distribution, and bioavailability in the North Pacific Ocean: Insights from data and models. *Global Biogeochem. Cy.* **2009**, *23*(2), 14 p ; DOI 10.1029/2008gb003425
- ⁹³ Munson, K. M.; Lamborg, C. H.; Swarr, G. J., Saito, M. A. Mercury species concentrations and fluxes in the Central Tropical Pacific Ocean. *Global Biogeochem. Cy.* **2015**, *29* ; DOI 10.1002/2015GB005120.
- ⁹⁴ Cossa, D.; Heimbürger, L. E.; Lannuzel, D.; Rintoul, S. R.; Butler, E. C. V.; Bowie, A. R.; Averty, B.; Watson, R. J.; Remenyi, T. Mercury in the Southern Ocean. *Geochim. Cosmochim. Acta* **2011**, *75*, 4037–4052 ; DOI 10.1016/j.gca.2011.05.001.
- ⁹⁵ Heimbürger-Boavida, L.E. Mediterranean Institute of Oceanography, Université Aix-Marseille, France. unpublished results from GEOVIDE-GEOTRACES cruise.

-
- ⁹⁶ Mason, R. P.; Fitzgerald, W. F. Alkylmercury species in the equatorial Pacific. *Nature* **1990**, 347(6292), 457-459 ; DOI 10.1038/347457a0.
- ⁹⁷ Cossa, D.; Averty, B.; Pirrone, N. The origin of methylmercury in open Mediterranean waters. *Limnol. Oceanogr.* **2009**, 54, 837-844 ; DOI 10.4319/lo.2009.54.3.0837.
- ⁹⁸ Blum, J. D.; Popp, B. N.; Drazen, J. C.; Choy, C. A.; Johnson, M. W. Methylmercury production below the mixed layer in the North Pacific Ocean. *Nat. Geosci.* **2013**, 6, 879-884 ; DOI 10.1038/NGEO1918.
- ⁹⁹ Kotnik, J.; Sprovieri, F.; Ogrinc, N.; Horvat, M.; Pirrone, N. Mercury in the Mediterranean, part I: spatial and temporal trends. *Environ. Sci. Pollut. Res.* **2014**, 21, 4063-4080 ; DOI 10.1007/s11356-013-2378-2.
- ¹⁰⁰ Gascon Diez, E.; Loizeau, J.-L.; Cosio, C.; Bouchet, S.; Adatte, T.; Amouroux D., Bravo, A. Role of Settling Particles on Mercury Methylation in the Oxidic Water Column of Freshwater Systems. *Environ. Sci. Technol.* **2016**, 50, 11672-11679 ; DOI 10.1021/acs.est.6b03260.
- ¹⁰¹ Munson, K. M.; Lamborg, C. H.; Boiteau, R. M.; Saito, M. A. Dynamic mercury methylation and demethylation in oligotrophic marine water. *Biogeosciences* **2018**, 15, 6451-6460 ; DOI 10.5194/bg-15-6451-2018.
- ¹⁰² Rizzo, A. L.; Caracausi, A.; Chavagnac, V.; Nomikou, P.; Polymenakou, P. N.; Mandalakis, M.; Kotoulas, G.; Magoulas, A.; Castillo, A.; Lampridou, D.; Maruszczak, N.; Sonke J. E. Geochemistry of CO₂-Rich Gases Venting from Submarine Volcanism: The Case of Kolumbo (Hellenic Volcanic Arc, Greece). *Front. Earth Sci.* **2019**, 7, 60 ; DOI 10.3389/feart.2019.00060.
- ¹⁰³ Heimbürger, L. E.; Cossa, D.; Thibodeau, B.; Khripounoff, A.; Mas, V.; Chiffolleau, J.-F.; Schmidt, S.; Migon, C. Natural and anthropogenic trace metals in sediments of the Ligurian Sea (Northwestern Mediterranean). *Chem. Geol.* **2012**, 291, 141-151 ; DOI 10.1016/j.chemgeo.2011.10.011.
- ¹⁰⁴ Ogrinc, N.; Hintelmann, H.; Kotnik, J.; Horvat, M.; Pirrone, N. Sources of mercury in deep-sea sediments of the Mediterranean Sea as revealed by mercury stable isotopes. *Sci. Rep.* **2019**, 9, 11626 ; DOI 10.1038/s41598-019-48061-z.
- ¹⁰⁵ Cossa, D.; Mucci, A.; Guédron, S.; Coquery, M.; Radakovitch, O.; Escoube, R.; Campillo, S.; Heussner, S. Mercury accumulation in the sediment of the Western Mediterranean abyssal plain: A reliable archive of the late Holocene. *Geochim. Cosmochim. Acta*, **309**, 1-15 ; DOI 10.1016/j.gca.2021.06.014.
- ¹⁰⁶ Coquery, M. INRAE, Lyon, France. Unpublished results from ADIOS project.
- ¹⁰⁷ ADIOS Final Report. *Atmospheric deposition and Impact of Pollutants, key elements, and nutrients on the open Mediterranean Sea*. Section 6: detailed report related to overall project duration; 2004; pp 93; European Communities; Contract number: EVK3-CT-2000-00035 Coordinator: S. Heussner (CNRS, France); www.Cordis.europa.eu/project/id/EVK3-CT-2000-00035/results.
- ¹⁰⁸ Živković, I.; Kotnik, J.; Šolić, M.; Horvat, M. The abundance, distribution and speciation of mercury in waters and sediments of the Adriatic Sea – a review. *Acta Adriat.* **2017**, 58, 165-186.
- ¹⁰⁹ Durrieu de Madron, X.; Wiberg, P. L.; Puig, P. Sediment dynamics in the Gulf of Lions: The impact of Extreme events. Introduction. *Cont. Shelf Res.* **2008**, 28, 1967-1876 ; DOI 10.1016/j.csr.2008.08.001.
- ¹¹⁰ Cossa, D.; Heimbürger, L.-E.; Pérez, F. F.; García-Ibáñez, M. I.; Sonke, J. E.; Planquette, H.; Lherminier, P.; Boutorh, J.; Cheize, M.; Menzel Barraqueta, J. L.; Shelley R.; Sarthou, G. Mercury distribution and transport in the North Atlantic Ocean along the Geotraces-GA01 transect. *Biogeosciences* **2018**, 15(8), 2309-2323 ; DOI:10.5194/bg-15-2309-2018.
- ¹¹¹ Migon, C.; Heimbürger-Boavida, L.-E.; Dufour, A.; Chiffolleau, J.-F.; Cossa D. Temporal variability of dissolved trace metals at the DYFAMED time-series station, Northwestern Mediterranean. *Mar. Chem.* **2020**, 225, 103846 ; DOI 10.1016/j.marchem.2020.103846.
- ¹¹² Huertas, I. E.; A. F. Ríos, A. F.; García-Lafuente, J.; Navarro, G.; Makaoui, A.; Sánchez-Román, A.; Rodríguez-Galvez, S.; Orbi, A.; Ruíz, J.; Pérez, F. F. Atlantic forcing of the Mediterranean oligotrophy, *Global Biogeochem. Cy.* **2012**, 26, GB2022 ; DOI 10.1029/2011GB004167.
- ¹¹³ Castagna, J.; Bencardino, M.; d'Amore, F.; Esposito, G.; Pirrone, N.; Sprovieri, F. Atmospheric mercury species measurements across the Western Mediterranean region: Behaviour and variability

-
- during a 2015 research cruise campaign. *Atmos. Environ.* **2018**, *173*, 108–126 ; DOI 10.1016/j.atmosenv.2017.10.045.
- ¹¹⁴ Bagnato, E.; Aiuppa, A.; Parello, F.; Allard, P.; Liuzzo, M.; Giudice, G.; Shinohara, H. New clues on mercury contribution from Earth volcanism. *Bull. Volcanol.* **2011**, *73*, 497–510.
- ¹¹⁵ Bagnato, E.; Aiuppa, A.; Parello, F.; Calabrese, S.; D'Alessandro, W.; Mather, T. A.; McGonigle, A. J. S.; Pyle, D. M.; Wängberg, I., 2007. Degassing of gaseous (elemental and reactive) and particulate mercury from Mount Etna volcano (Southern Italy). *Atmos. Environ.* **2007**, *41*, 7377–7388 ; DOI 10.1016/j.atmosenv.2007.05.060.
- ¹¹⁶ Bagnato, E.; Tamburello, G.; Avard, G.; Martinez-Cruz, M.; Enrico, M.; Fu, X.; Sprovieri, M.; Sonke, J. E. Mercury Fluxes from Volcanic and Geothermal Sources: An Update. *Geol. Soc. Lond. Spec. Publ.* **2015**, *410*, 263–285 ; DOI 10.1144/SP410.2.
- ¹¹⁷ Carn, S. A.; Fioletov, V. E.; McLinden, C. A.; Li, C.; Krotkov, N. A. A Decade of Global Volcanic SO₂ Emissions Measured from Space. *Sci. Rep.* **2017**, *7*, 44095 ; DOI.org/10.1038/srep44095.
- ¹¹⁸ Bowman, K. L.; Hammerschmidt, C. R.; Lamborg, C. H.; Swarr, G. Mercury in the North Atlantic Ocean: the U.S. GEOTRACES zonal and meridional sections. *Deep-Sea Res. II* **2015**, *116*, 251–261.
- ¹¹⁹ Bratkič, A.; M. Vahčić, M.; Kotnik, J.; Obu Vazner, K.; Begu, E.; Woodward, E. M. S. Horvat, M. Mercury presence and speciation in the South Atlantic Ocean along the 40°S transect, *Global Biogeochem. Cy.* **2016**, *30*, 105–119 ; DOI 10.1002/2015GB005275.
- ¹²⁰ Panagos, P.; Jiskra, M.; Borrelli, P.; Liakos, L.; Ballabio, C. Mercury in European topsoils: Anthropogenic sources, stocks and fluxes. *Environ. Res.* **2021**, *201*, 111556 ; DOI 10.1016/j.envres.2021.111556.
- ¹²¹ Bouraoui, F.; Grizzetti, B.; Aloe, A. Estimation of water fluxes into the Mediterranean Sea. *J. Geophys. Res.* **2010**, *115*, D21116 ; DOI:10.1029/2009JD013451.
- ¹²² Shaltout, M.; Omstedt, A. Calculating the water and heat balances of the Eastern Mediterranean Basin using ocean modelling and available meteorological, hydrological and ocean data. *Oceanologia* **2012**, *54*, 199–232 ; DOI:10.597/oc.54-2.199.
- ¹²³ Shaltout, M.; Omstedt, A. Modelling the water and heat balances of the Mediterranean Sea using a two-basin model and available meteorological, hydrological, and ocean data. *Oceanologia* **2015**, *57*, 116–131 ; DOI 10.1016/j.oceano.2014.11.001.
- ¹²⁴ Petrova, M. V. Mediterranean Institute of Oceanography, Université Aix-Marseille, France
- ¹²⁵ Trezzi, G.; Garcia-Orellana, J.; Rodellas, V.; Santos-Echeandia, J.; Tovar-Sánchez, A.; Garcia-Solsona, E.; Masqué, P. Submarine groundwater discharge: A significant source of dissolved trace metals to the North Western Mediterranean Sea. *Mar. Chem.* **2016**, *186*, 90–100.
- ¹²⁶ Salvagio Manta, D.; Bonsignore, M.; Oliveri, E.; Barra, M.; Tranchida, G.; Giaramita, L.; Mazzola, S.; Sprovieri, M. Fluxes and the mass balance of mercury in Augusta Bay (Sicily, southern Italy). *Estuar. Coast. Shelf Sci.* **2016**, *181*, 134–143 ; DOI 10.1016/j.ecss.2016.08.01.
- ¹²⁷ Eakins, B. W.; Sharman, G. F. *Volumes of the World's Oceans from ETOPO1*, NOAA National Geophysical Data Center, Boulder, CO, 2010; www.ngdc.noaa.gov/mgg/global/etopo1_ocean_volumes.html.
- ¹²⁸ Gilmour, C. C.; Podar, M.; Bullock, A. L.; Graham, A. M.; Brown, S. D.; Somenahally, A. C.; Johs, A.; Hurt, R. A.; Bailey, K. L.; Elias, D. A. Mercury methylation by novel microorganisms from new environments. *Environ. Sci. Technol.* **2013**, *47*, 11810–11820 ; DOI 10.1021/es403075t.
- ¹²⁹ Parks, J. M.; Johs, A.; Podar, M.; Bridou, R.; Hurt, R. A.; Smith, S. D.; Tomanicek, S. J.; Qian, Y.; Brown, S. D.; Brandt, C. C.; Palumbo, A. V.; Smith, J. C.; Wall, J. D.; Elias, D. A.; Liang, L. The genetic basis for bacterial mercury methylation. *Science* **2013**, *339*, 1332–1335 ; DOI 10.1126/science.1230667.
- ¹³⁰ Podar, M.; Gilmour, C. C.; Brandt, C. C.; Soren, A.; Brown, S. D.; Crable, B. R.; Palumbo, A. V.; Somenahally, A. C.; Elias, D. A. Global prevalence and distribution of genes and microorganisms involved in mercury methylation. *Sci. Adv.* **2015**, *1*, e1500675–e1500675 ; DOI 10.1126/sciadv.1500675.
- ¹³¹ Gionfriddo, C. M.; Tate, M. T.; Wick, R. R.; Schultz, M. B.; Zemla, A.; Thelen, M. P.; Schofield, R.; Krabbenhoft, D. P.; Holt, K. E.; Moreau, J. W. Microbial mercury methylation in Antarctic sea ice.

-
- Nat. Microbiol.* **2016**, *1*, 16127 ; DOI 10.1038/nmicrobiol.2016.127.
- ¹³² Villar, E.; Cabrol, L.; Heimbürger-Boavida, L.-E. Widespread microbial mercury methylation genes in the global ocean. *Environ. Microbiol. Rep.* **2020**, *12*(3), 277-287 ; DOI 10.1111/1758-2229.12829.
- ¹³³ Mason, R. P.; Lawson, N. M.; Sheu, G. Mercury in the Atlantic Ocean: factors controlling air – sea exchange of mercury and its distribution in the upper waters. *Deep Sea Res. Part II* **2001**, *48*, 2829–2853 ; DOI 10.1016/S0967-0645(01)00020-0.
- ¹³⁴ Barkay, T.; Miller, S. M.; Summers, A. O. 2003. Bacterial mercury resistance from atoms to ecosystems. *FEMS Microbiol. Rev.* **2003**, *27*, 355–384 ; DOI 10.1016/S0168-6445(03)00046-9.
- ¹³⁵ Zhang, T.; Hsu-kim, H. Photolytic degradation of methylmercury enhanced by binding to natural organic ligands. *Nat. Geosci.* **2010**, *3*, 473–476 ; DOI 10.1038/ngeo892.
- ¹³⁶ Costa, M.; Liss, P. S. Photoreduction of mercury in sea water and its possible implications for Hg 0 air–sea fluxes. *Mar. Chem.* **1999**, *68*, 87–95 ; DOI 10.1016/S0304-4203(99)00067-5.
- ¹³⁷ Qureshi, A.; O’Driscoll, N. J.; Macleod, M.; Neuhold, Y. M.; Hungerbühler, K. Photoreactions of mercury in surface ocean water: Gross reaction kinetics and possible pathways. *Environ. Sci. Technol.* **2010**, *44*, 644–649 ; DOI 10.1021/es9012728
- ¹³⁸ Black, F. J.; Poulin, B. A.; Flegal, A. R. Factors controlling the abiotic photo-degradation of monomethylmercury in surface waters. *Geochim. Cosmochim. Acta* **2012**, *84*, 492–507. DOI 10.1016/j.gca.2012.01.019.
- ¹³⁹ Marvin-Dipasquale, M.; Agee, J.; McGowan, C.; Oremland, R. S.; Thomas, M.; Krabbenhoft, D.; Gilmour, C. Methyl-Mercury Degradation Pathways: A Comparison among Three Mercury-Impacted Ecosystems. *Environ. Sci. Technol.* **2000**, *34*, 4908-4916 ; DOI 10.1021/es0013125.
- ¹⁴⁰ Bowman, K. L.; Collins, R. E.; Agather, A.M.; Lamborg, C. H.; Hammerschmidt, C. R.; Kaul, D.; Dupont, C. L.; Christensen, G. A.; Elias, D. A. Distribution of mercury-cycling genes in the Arctic and equatorial Pacific Oceans and their relationship to mercury speciation. *Limnol. Oceanogr.* **2020**, *65*, S310–S320 ; DOI 10.1002/lno.11310.
- ¹⁴¹ Baya, P. A.; Gosselin M.; Lehnher I.; St. Louis V. L.; Hintelmann, H. Determination of monomethylmercury and dimethylmercury in the arctic marine boundary layer. *Environ. Sci. Technol.* **2015**, *49*, 223-232 ; DOI 10.1021/es502601z.
- ¹⁴² Jonsson, S.; Mazrui, N. M.; Mason, R. P. Dimethylmercury Formation Mediated by Inorganic and Organic Reduced Sulfur Surfaces. *Sci. Rep.* **2016**, *6*, 27958 ; DOI 10.1038/srep27958.
- ¹⁴³ Storelli, M.; Marcotrigiano, G. Total mercury levels in muscle tissue of swordfish (*Xiphias gladius*) and bluefin tuna (*Thunnus thynnus*) from the Mediterranean sea (Italy). *Food. Prot.* **2001**, *64*, 1058-1061.
- ¹⁴⁴ Storelli, M.; Giacomini-Stuffler, R. ; Storelli, A. ; Marcotrigiano, G. Accumulation of mercury, cadmium, lead and arsenic in swordfish and bluefin tuna from Mediterranean Sea : a comparative study. *Mar. Pollut. Bull.* **2005**, *50*, 1004-1007.
- ¹⁴⁵ Abolghait S. K.; Garbaj A. M. Determination of cadmium, lead and mercury residual levels in meat of canned light tuna (*Katsuwonus pelamis* and *Thunnus albacares*) and fresh little tunny (*Euthynnus alletteratus*) in Libya. *Open Vet. J.* **2015**, *5*, 130-137.
- ¹⁴⁶ Annibaldi, A.; Truzzi, C.; Carnevali, O.; Pignatola, P.; Api, M.; Scarponi, G.; Silvia Illuminati S. 2019. Determination of Hg in farmed and wild Atlantic Bluefin tuna (*Thunnus thynnus* L.) muscle. *Molecules* **2019**, *24*(7), 1273. DOI 10.3390/molecules24071273.
- ¹⁴⁷ Barone, G.; Dambrosio, A.; Storelli, A.; Garofalo, R.; Busco, V. P.; Storelli M. M. 2018. Estimated Dietary Intake of Trace Metals from Swordfish Consumption: A Human Health Problem. *Toxics* **2018**, *6*, 22. DOI 10.3390/toxics6020022.
- ¹⁴⁸ Cinnirella, S.; Bruno, D. E.; Pirrone, N.; Horvat, M.; Živković, I.; Evers, D. C.; Johnson, S.; Sunderland, E. M. Mercury concentrations in biota in the Mediterranean Sea, a compilation of 40 years of surveys. *Sci. Data* **2019**, *6*, 205 ; DOI 10.1038/s41597-019-0219-y.
- ¹⁴⁹ Esposito, M.; De Roma, A.; La Nuera, R.; Picazio, G.; Gallo, P. Total mercury content in commercial swordfish (*Xiphias gladius*) from different FAO fishing areas. *Chemosphere* **2018**, *197*, 14-19 ; DOI 10.1016/j.chemosphere.2018.01.015.

-
- ¹⁵⁰ Lee, C. S.; Fisher, N. S. Bioaccumulation of methylmercury in a marine copepod. *Environ. Toxicol. Chem.* **2016**, *9999*, 1-7 ; DOI 10.1002/etc.3660.
- ¹⁵¹ Mason, R. P.; Reinfelder, J. R.; Morel, F. M. F. Uptake, Toxicity, and Trophic Transfer of Mercury in a Coastal Diatom Uptake, Toxicity, and Trophic Transfer of Mercury in a Coastal Diatom. *Environ. Sci. Technol.* **1996**, *30*, 1835-1845 ; DOI 10.1021/es950373d.
- ¹⁵² Lee, C. S.; Fisher, N. S. Bioaccumulation of methylmercury in a marine diatom and the influence of dissolved organic matter. *Mar. Chem.* **2017**, *197*, 70-79 ; DOI 10.1016/j.marchem.2017.09.005.
- ¹⁵³ Harding, G.; Dalziel, J.; Vass, P. Bioaccumulation of methylmercury within the marine food web of the outer Bay of Fundy, Gulf of Maine. *PLoS ONE* **2018**, *13*, e0197220 ; DOI 10.1371/journal.pone.0197220.
- ¹⁵⁴ Hunt, B. P. V.; Carlotti, F.; Donoso, K.; Pagano, M.; D'Ortenzio, F.; Taillandier, V.; Conan, P. Trophic pathways of phytoplankton size classes through the zooplankton food web over the spring transition period in the north-west Mediterranean Sea. *J. Geophys. Res. Oceans* **2017**, *122*, 6309-6324 ; DOI:10.1002/2016JC012658.
- ¹⁵⁵ Barbieux, M.; Uitz, J.; Gentili, B.; Pasqueron de Fommervault, O.; Mignot, A.; Poteau, A.; Schmechtig, C.; Taillandier, V.; Leymarie, E.; Penkerc'h, C.; D'Ortenzio, F.; Claustre, H.; Bricaud, A. Bio-optical characterization of subsurface chlorophyll maxima in the Mediterranean Sea from a Biogeochemical-Argo float database. *Biogeosciences* **2019**, *16*, 1321-1342 ; DOI 10.5194/bg-16-1321-2019.
- ¹⁵⁶ Harmelin-Vivien, M.; Cossa, D.; Crochet, S.; Banaru, D.; Letourneur, Y.; Mellon-Duval, C. Difference of mercury bioaccumulation in red mullets from the north-western Mediterranean and Black seas. *Mar. Pollut. Bull.* **2009**, *58*, 679-685 ; DOI 10.1016/j.marpolbul.2009.01.004.
- ¹⁵⁷ Chouvelon, T.; Strady, E.; Harmelin-Vivien, M.; Radakovitch, O.; Brach-Papa, C.; Crochet, S.; Knoery, J.; Rozuel, E.; Thomas, B.; Tronczynski, J.; Chiffolleau, J.-F. Patterns of trace metal bioaccumulation and trophic transfer in a phytoplankton-zooplankton-small pelagic fish marine food web. *Mar. Pollut. Bull.* **2019**, *146*, 1013-1030 ; DOI 10.1016/j.marpolbul.2019.07.047.
- ¹⁵⁸ Zhang, Y.; Soerensen, A. L.; Schartup, A. T.; Sunderland, E. M. A global model for methylmercury formation and uptake at the base of marine food webs. *Global Biogeochem. Cy.* **2020**, *34*, e2019GB006348 ; DOI 10.1029/2019GB006348.
- ¹⁵⁹ Twining, B. S.; Fisher, N. S. Trophic transfer of trace metals from protozoa to mesozooplankton. *Limnol. Oceanogr.* **2004**, *49*, 2004, 28-39.
- ¹⁶⁰ Fisk, A. T.; Hobson, K. A.; Norstrom, R. J. Influence of chemical and biological factors on trophic transfer of persistent organic pollutants in the Northwater Polynia marine food web. *Environ. Sci. Technol.* **2001**, *35*, 732-738 ; DOI 10.1021/es001459w.
- ¹⁶¹ Mathews, T.; Fisher, N. S. Dominance of dietary intake of metals in marine elasmobranch and teleost fish. *Sci. Tot. Environ.* **2009**, *407*, 5156-5161 ; DOI 10.1016/j.scitotenv.2009.06.003.
- ¹⁶² Joiris, C. R.; Holsbeek, L.; Laroussi Moatemri, N. Total and methylmercury in sardines *Sardinella aurita* and *Sardina pilchardus* from Tunisia. *Mar. Pollut. Bull.* **1999**, *38*, 188-192 ; DOI.org/10.1016/S0025-326X(98)00171-4.
- ¹⁶³ Stacy, W. L.; Lepak, J. M. Relative influence of prey mercury concentration, prey energy density and predator sex on sport fish mercury concentrations. *Sci. Total Environ.* **2012**, *437*, 104-109 ; DOI 10.1016/j.scitotenv.2012.07.064.
- ¹⁶⁴ Pinzone, M.; Damseaux, F.; Michel, L. N.; Das, K. Stable isotope ratios of carbon, nitrogen and sulphur and mercury concentrations as descriptors of trophic ecology and contamination sources of Mediterranean whales. *Chemosphere* **2019**, *237*, 124448 ; DOI 10.1016/j.chemosphere.2019.124448.
- ¹⁶⁵ Costantini, D.; Bustamante, P.; Brault-Favrou, M.; Dell'Omo, G. Patterns of mercury exposure and relationships with isotopes and markers of oxidative status in chicks of a Mediterranean seabird. *Environ. Pollut.* **2020**, *260*, 114095 ; DOI 10.1016/j.envpol.2020.114095.
- ¹⁶⁶ Bouchoucha, M.; Chekri, R.; Leufroy, A.; Jitaru, P.; Millour, S.; Marchond, N.; Chafrey, C.; Testu, C.; Zinck, J.; Cresson, P.; Mirallès, F.; Mahe, A.; Arnich, N.; Sanaa, M.; Bemrah, N.; Guérin, T. Trace

-
- element contamination in fish impacted by bauxite red mud disposal in the Cassidaigne canyon (NW French Mediterranean). *Sci. Total Environ.* **2019**, *690*, 16-26 ; DOI 10.1016/j.stotenv.2019.06.474.
- ¹⁶⁷ Maulvault, A. L.; Custódio, A.; Anacleto, P.; Repolho, T.; Pousão, P.; Nunes, M. L.; Diniz, M.; Rosa, R.; Marques, A. Bioaccumulation and elimination of mercury in juvenile seabass (*Dicentrarchus labrax*) in a warmer environment. *Environ. Res.* **2016**, *149*, 77-85 ; DOI 10.1016/j.envres.2016.04.035.
- ¹⁶⁸ Sánchez-Muros, M. J.; Morote, E.; Gil, C.; Ramos-Miras Torrijos, M.; Rodríguez Martín, J. A. Mercury contents in relation to biometrics and proximal composition and nutritional levels of fish eaten from the Western Mediterranean Sea (Almería bay). *Mar. Pollut. Bull.* **2018**, *135*, 783-789 ; DOI 10.1016/j.marpolbul.2018.08.003.
- ¹⁶⁹ Branco, V.; Vale, C.; Canário, J.; Neves dos Santos, M. Mercury and selenium in blue shark (*Prionace glauca*, L. 1758) and swordfish (*Xiphias gladius*, L. 1758) from two areas of the Atlantic Ocean. *Environ. Pollut.* **2007**, *150*, 373-380 ; DOI 10.1016/j.envpol.2007.01.040.
- ¹⁷⁰ Cresson, P.; Bouchoucha, M.; Morat, F.; Miralles, F.; Chavanon, F.; Loizeau, V.; Cossa, D. A multitracer approach to assess the spatial contamination pattern of hake (*Merluccius merluccius*) in the French Mediterranean. *Sci. Total Environ.* **2015**, *532*, 184-194 ; DOI 10.1016/j.scitotenv.2015.06.020.
- ¹⁷¹ Harmelin-Vivien, M.; Bodiguel, X.; Charmasson, S.; Loizeau, V.; Mellon-Duval, C.; Tronczyński, J.; Cossa, D. Differential biomagnification of PCB, PBDE, Hg and Radiocesium in the food web of the European hake from the NW Mediterranean. *Mar. Pollut. Bull.* **2012**, *64*, 974-983 ; DOI 10.1016/j.marpolbul.2012.02.014.
- ¹⁷² Capelli, R.; Drava G.; Siccardi C.; De Pellegrini R.; Minganti V., 2004. Study of the distribution of trace elements in six species of marine organisms of the Ligurian Sea (North-Western Mediterranean). Comparison with previous findings. *Annali di Chimica* **2004**, *94*, 533-546 ; DOI 10.1002/adic.200490067.
- ¹⁷³ Cresson, P.; Fabri, M.-C.; Bouchoucha, M.; Brach Papa, C.; Chavanon, F.; Jadaud, A.; Knoery, J.; Miralles, F.; Cossa D. Mercury in organisms from the Northwestern Mediterranean slope: importance of food sources. *Sci. Total Environ.* **2014**, *497-498*, 229-238 ; DOI 10.1016/j.scitotenv.2014.07.069.
- ¹⁷⁴ Storelli, M. M.; Storelli, A.; Giacomini-Stuffler, R.; Marcotrigiano, G. O. Mercury speciation in the muscle of two commercially important fish, hake (*Merluccius merluccius*) and striped mullet (*Mullus barbatus*) from the Mediterranean Sea: estimated weekly intake. *Food Chem.* **2005**, *89*, 295-300 ; DOI 10.1016/j.foodchem.2004.02.036.
- ¹⁷⁵ Signa, G.; Mazzola, A.; Tramati, C. D.; Vizzini, S. Diet and habitat use influence Hg and Cd transfer to fish and consequent biomagnification in a highly contaminated area: Augusta Bay (Mediterranean Sea). *Environ. Pollut.* **2017**, *230*, 394-404 ; DOI 10.1016/j.envpol.2017.06.027.
- ¹⁷⁶ Grgec, A. S.; Kljaković-Gašpić, Z.; Orct, T.; Tičina, V.; Sekovanić, A.; Jurasović, J.; Piasek, M. Mercury and selenium in fish from the eastern part of the Adriatic Sea: A risk-benefit assessment in vulnerable population groups. *Chemosphere* **2020**, *261*, 127742 ; DOI 10.1016/j.chemosphere.2020.127742.
- ¹⁷⁷ Ourgaud, M. Influence des apports anthropiques sur les flux de carbone et de contaminants dans les réseaux trophiques de 'poissons' de l'écosystème à Posidonia oceanica. Ph. D. Dissertation, Aix-Marseille University, France ; 2015 pp 350 ; www.theses.fr/2015AIXM4097.
- ¹⁷⁸ Ourgaud, M.; Ruitton, S.; Bourgogne, H.; Bustamante, P.; Churlaud, C.; Guillou, G.; Lebreton, B.; Harmelin-Vivien, M. Trace elements in a Mediterranean scorpaenid fish: bioaccumulation processes and spatial variations. *Progr. Oceanogr.* **2018**, *163*, 184-195 ; DOI 10.1016/j.pocan.2017.11.008.
- ¹⁷⁹ Chouvelon, T.; Spitz, J.; Caurant, F.; Mendez-Fernandez, P.; Autier, J.; Lassus-Debat, A.; Bustamante, P. Enhanced bioaccumulation of mercury in deep-sea fauna from the Bay of Biscay (North-East Atlantic) in relation to trophic positions identified by analysis of carbon and nitrogen stable isotopes. *Deep-Sea Res. I* **2012**, *65*, 113-124 ; DOI 10.1016/j.dsr.2012.02.010.
- ¹⁸⁰ Cransveld, A.; Amouroux, D.; Tessier, E.; Koutrakis, E.; Ozturk, A. A.; Bettoso, N.; Mieiuro, C. L.; Bérail, S.; Barre, J. P. G.; Sturaro, N.; Schnitzler, J.; Das K. Mercury stable isotopes discriminate different populations of European seabass and trace potential Hg sources around Europe. *Environ. Sci. Technol.* **2017**, *51*, 12219-12228 ; DOI 10.1021/acs.est.7b01307.

-
- ¹⁸¹ Buckman, K. L.; Lane, O.; Kotnik, J.; Bratkic, A.; Sprovieri, F.; Horvat, M.; Pirrone, N.; Evers, D. C.; Chen, C. Y. Spatial and taxonomic variation of mercury concentration in low trophic level fauna from the Mediterranean Sea. *Ecotoxicology* **2018**, *27*, 1341-1352 ; DOI 10.1007/s10646-018-1986-5.
- ¹⁸² Orani, A. M.; Vassileva, E.; Azemard, S.; Thomas, O. P. Comparative study on Hg bioaccumulation and biotransformation in Mediterranean and Atlantic sponge species. *Chemosphere* **2020**, *260*, 127515 ; DOI 10.1016/j.chemosphere.2020.127515.
- ¹⁸³ Kucuksezgin, F.; Altay, O.; Uluturhan, E.; Kontas, A. Trace metal and organochlorine residue levels in red mullet (*Mullus barbatus*) from the Eastern Aegean, Turkey. *Wat. Res.* **2001**, *35*, 2327-2332 ; DOI 10.1016/S0043-1354(00)00504-2.
- ¹⁸⁴ Briant, N.; Chouvelon, T.; Martinez, L.; Brach-Papa, C.; Chiffolleau, J.-F.; Savoye, N.; Sonke, J.; Knoery, J. Spatial and temporal distribution of mercury and methylmercury in bivalves from the French coastline. *Mar. Pollut. Bull.* **2017**, *114*, 1096-1102 ; DOI 10.1016/j.marpolbul.2016.10.018.
- ¹⁸⁵ Remen, M.; Nederlof, M. A. J.; Folkedal, O.; Thorsheim, G.; Sitja-Bobadilla, A.; Pérez-Sánchez, J.; Oppedal, F.; Olsen, R. E. Effect of temperature on the metabolism, behavior and oxygen requirements of *Sparus aurata*. *Aquacult. Environ. Interact.* **2015**, *7*, 115-123 ; DOI 10.3354/aei00141.
- ¹⁸⁶ Neubauer, P.; Andersen K. H. Thermal performance of fish is explained by an interplay between physiology, behaviour and ecology. *Conserv. Physiol.* **2019**, *7*, coz025. Doi:10.1093/conphys/coz025.
- ¹⁸⁷ Silva, A.; Carrera, P.; Massé, J.; Uriarte, A.; Santos, M. B.; Oliveira, P. B.; Soares, E.; Porteiro, C. Y.; Stratoudakis, Y. Geographic variability of sardine growth across the northeastern Atlantic and the Mediterranean Sea. *Fish. Res.* **2008**, *90*, 56-69 ; DOI 10.1016/j.fishres.2007.09.011.
- ¹⁸⁸ Mellon-Duval, C.; de Pontual, H.; Métral, L.; Quemener, L. Growth of European hake (*Merluccius merluccius*) in the Gulf of Lions based on conventional tagging. *ICES J. Mar. Sci.* **2009**, *67*, 62-70 ; DOI 10.1093/icesjms/fsp215.
- ¹⁸⁹ Lavoie, R. A.; Jardine, T. D.; Chumchal, M. M.; Kidd, K. A.; Campbell, L. M. Biomagnification of mercury in aquatic food webs: a worldwide meta-analysis. *Environ. Sci. Technol.* **2013**, *47*, 13385-13394 ; DOI 10.1021/es403103t.
- ¹⁹⁰ Borgå, K.; Kidd, K. A.; Muir, D. C. G.; Berglund, O.; Conder, J. M.; Gobas, F. A. P. C.; Kucklick, J.; Malm, O.; Powell, D. E. Trophic magnification factors: considerations of ecology, ecosystems, and study design. *Integr. Environ. Assess. Manag.* **2011**, *8*, 64-84 ; DOI 10.1002/jeam.244.
- ¹⁹¹ Alava, J. J.; Cheung W. W. L.; Ross P. S.; Sumaila R. U. Climate change-contaminant interactions in marine food webs: Towards a conceptual framework. *Glob. Change Biol.* **2017**, *23*, 3984-4001 ; DOI 10.1111/gcb.13667.
- ¹⁹² Du Pontavice, H.; Gascuel, D.; Reygondeau, G.; Maureaud, A.; Cheung W. W. L. 2020, Climate change undermines the global functioning of marine food webs. *Glob. Change Biol.* **2020**, *26*, 1306-1318 ; DOI 10.1111/gcb.14944.
- ¹⁹³ Cresson, P.; Chouvelon, T.; Bustamante, P.; Bănar, D.; Baudrier, J.; Le Loc'h, F.; Mauffret, A.; Mialet, B.; Spitz, J.; Wessel, N.; Briand, M.; Denamiel, M.; Doray, M.; Guillou, G.; Jadaud, A.; Lazard, C.; Petit, L.; Prieur, S.; Rouquette, M.; Saraux, C.; Serre, S.; Timmerman, C.A.; Verin, Y.; Harmelin-Vivien, M., 2020. Primary production and depth drive different trophic structure and functioning of fish assemblages in French marine ecosystems. *Progr. Oceanogr.* **2020**, *186*, 102343 ; DOI 10.1016/j.pocean.2020.102343.
- ¹⁹⁴ Christensen, V.; Walters, C. J. Ecopath with Ecosim: methods, capabilities and limitations. *Ecol. Model.* **2004**, *172*, 109-139 ; DOI 10.1016/j.ecolmodel.2003.09.003.
- ¹⁹⁵ Christensen, V.; Walters, C. J.; Pauly, D. *Ecopath with Ecosim: A User's Guide*. Fisheries Centre, University of British Columbia, Vancouver, Canada, pp 154; 2005.
- ¹⁹⁶ Piroddi, C.; Coll, M.; Liqueste, C.; Macias, D. M.; Greer, K.; Buszowski, J.; Steenbeek, J.; Danovaro, R.; Christensen, V. Historical changes of the Mediterranean Sea ecosystem: modelling the role and impact of primary productivity and fisheries changes over time. *Sci. Rep.* **2017**, *7*, 44491 ; DOI 10.1038/srep44491
- ¹⁹⁷ Outridge, P. M.; Macdonald R. W.; Wang F.; Stern G. A.; Dastoor A. P. A mass balance inventory of mercury in the Arctic Ocean. *Environ. Chem.* **2008**, *5*, 89-111 ; DOI 10.1071/EN08002.

-
- ¹⁹⁸ WHO (*World Health Organization*); 2017; www.who.int/news-room/fact-sheets/detail/mercury-and-health.
- ¹⁹⁹ Miklavčič Višnjevec, A.; Kocman, D.; Horvat, M. Human mercury exposure and effects in Europe. *Environ. Toxicol. Chem.* **2013**, *33*, 1259–1270 ; DOI 10.1002/etc.2482.
- ²⁰⁰ Basu, N.; Horvat, M.; Evers, D. C.; Zastenskaya, I.; Weihe, P.; Tempowski, J. A State-of-the-Science Review of Mercury Biomarkers in Human Populations Worldwide between 2000 and 2018. *Environ. Health Perspect.* **2019**, *126*, 106001-14 ; DOI 10.1289/EHP3904.
- ²⁰¹ Renzoni, A.; Zino, F.; Franchi, E. Mercury levels along the foodchain and risk for exposed populations. *Environ. Res.* **1997**, *77*, 68–72 ; DOI 10.1006/enrs.1998.3832.
- ²⁰² Cammilleri, G.; Vazzana, M.; Arizza, V.; Giunta, F.; Vella, A.; Lo Dico, G.; Giaccone, V.; Giofre, S. V.; Giangrosso, G.; Cicero, N.; Ferrantelli, V. Mercury in fish products: what's the best for consumers between bluefin tuna and yellowfin tuna? *Nat. Prod. Res.* **2018**, *32*(4), 457-462 ; DOI 10.1080/14786419.2017.1309538.
- ²⁰³ Bellanger, M.; Pichery, C.; Aerts, D.; Berglund, M.; Castaño, A.; Čejchanová, M.; Crettaz, P.; Davidson, F.; Esteban, M.; Fischer, M. E.; Gurzau, A. E.; Halzlova, K.; Katsonouri, A.; Knudsen, L. E.; Kolossa-Gehring, M.; Koppen, G.; Ligočka, D.; Miklavčič, A.; Reis, M. F.; Rudnai, P.; Tratnik, J. S.; Weihe, P.; Budtz-Jørgensen, E.; Grandjean, P.; DEMO/COPHES. Economic benefits of methylmercury exposure control in Europe: Monetary value of neurotoxicity prevention. *Environ. Health* **2013**, *12*, 3. DOI 10.1186/1476-069X-12-3.
- ²⁰⁴ Den Hond, E.; Govarts, E.; Willems, H.; Smolders, R.; Casteleyn, L.; Kolossa-Gehring, M.; Schwedler, G.; Seiwert, M.; Fiddicke, U.; Castaño, A.; Esteban, M.; Angerer, J. M.; Koch, H. K. Schindler, B.; Sepai, O.; Exley, K.; Bloemen, L.; Horvat, M.; Knudsen, L. E.; Joas, A.; Joas, R.; Biot, P.; Aerts, D.; Koppen, G.; Andromachi Katsonouri, A.; Hadjipanayis, A.; Krskova, A.; Maly, M.; Mørck, T.A.; Rudnai, P.; Kozepesy, S.; Mulcahy, M.; Mannion, R. C.; Gutleb, A. C. E.; Fischer, M. E.; Ligočka, D.; Jakubowski, M.; Reis, F.; Namorado, S.; Gurzau, A. E., Lupsa, I-R., Halzlova, Michal Jajcaj, M., Mazej, D., Snoj Tratnik, J., López, A.; Lopez, E.; Berglund, M.; Larsson, K.; Lehmann, A.; Crettaz, P.; Schoeters, G. First Steps toward Harmonized Human Biomonitoring in Europe: Demonstration Project to Perform Human Biomonitoring on a European Scale. *Environ. Health Perspect.* **2015**, *123*(3), 255-263 ; DOI 10.1289/ehp.1408616.
- ²⁰⁵ Ramon, R.; Murcia, M.; Aguinagalde, X.; Amurrio, A.; Llop, S.; Ibarluzea, J.; Lertxundi, A.; Alvarez-Pedrerol, M.; Casas, M.; Vioque, J.; Sunyer, J.; Tardon, A.; Martinez-Arguelles, B.; Ballester, F. Prenatal mercury exposure in a multicenter cohort study in Spain. *Environ. Int.* **2011**, *37*, 597-604 ; DOI 10.1016/j.envint.2010.12.004.
- ²⁰⁶ Mezghani-Chaari, S.; Hamza, A.; Hamza-Chaffai, A. Mercury contamination in human hair and some marine species from Sfax coasts of Tunisia: levels and risk assessment. *Environ. Monit. Assess.* **2011**, *180*, 477–487 ; DOI:10.1007/s10661-010-1800-1.
- ²⁰⁷ Miklavčič, A.; Casetta, A.; Snoj Tratnik, J.; Darja Mazej, D.; Krsnik, M.; Mariuz, M.; Sofianou, K.; Špirić, Z.; Barbone, F.; Horvat, M. Mercury, arsenic and selenium exposure levels in relation to fish consumption in the Mediterranean area. *Environ. Res.* **2013**, *120*, 7-17 ; DOI 10.1016/j.envres.2012.08.010.
- ²⁰⁸ Stratakis, N.; Conti, D. V.; Borrás, E.; Sabido, E.; Roumeliotaki, T.; Papadopoulou, E.; Agier, L.; Basagana, X.; Bustamante, M.; Casas, M.; Farzan, S. F.; Fossati, S.; Gonzalez, J. R.; Grazuleviciene, R.; Heude, B.; Maitre, L.; McEachan, R. R. C.; Theologidis, I.; Urquiza, J.; Vafeiadi, M.; West, J.; Wright, J.; McConnell, R.; Brantsaeter, A.-L.; Meltzer, H.-M.; Vrijheid, M.; Chatzi, L. Association of Fish Consumption and Mercury Exposure During Pregnancy with Metabolic Health and Inflammatory Biomarkers in Children. *JAMA Netw Open.* **2020**, *3*(3), e201007 ; DOI:10.1001/jamanetworkopen.2020.1007.
- ²⁰⁹ Barbone, F.; Rosolen, V.; Mariuz, M.; Parpinel, M.; Casetta, A.; Sammartano, F.; Ronfani, L.; Vecchi Brumatti L.; Bin, M.; Castriotta, L.; Valent, F.; Little, D. L.; Mazej, D.; Snoj Tratnik, J.; Miklavčič Višnjevec, A.; Sofianou, K.; Špirić, Z.; Krsnik, M.; Osredkar, J.; Neubauer, D.; Kodrič, J.; Stropnik, S.; Prpić, I.; Petrović, O.; Vlašić-Cicvarić, I.; Horvat, M. Prenatal mercury exposure and child neurodevelopment outcomes at 18 months: Results from the Mediterranean PHIME cohort. *Int. J. Hyg. Environ. Health.* **2019**, *222*(1), 9-21 ; DOI 10.1016/j.ijheh.2018.07.011.

-
- ²¹⁰ Llop, S.; Engström, K.; Ballester, F.; Franforte, E.; Alhamdow, A.; Pisa, F.; et al. Polymorphisms in ABC Transporter Genes and Concentrations of Mercury in Newborns – Evidence from Two Mediterranean Birth Cohorts. *PLoS ONE* **2014**, 9(5): e97172 ; DOI 10.1371/journal.pone.0097172.
- ²¹¹ Tranik, J. S.; Falnoga, I.; Trdin, A.; Mazej, D.; Fajon, V.; Miklavčič, A.; Kopal, A. B.; Osredkar, J.; Briški, A. S.; Krsnik, M.; Neubauer, D.; Kodrič, J.; Stropnik, S.; Gosar, D.; Musek, P. L.; Marc, J.; Mlakar, S. J.; Petrović, O.; Vlašić-Cicvarić, I.; Prpić, I.; Milardović, A.; Nišević, J. R.; Vuković, D.; Fišić, E.; Špirić, Z.; Horvat, M. Prenatal mercury exposure, neurodevelopment and apolipoprotein E genetic polymorphism. *Environ. Res.* **2017**, 152, 375-385 ; DOI 10.1016/j.envres.2016.08.035.
- ²¹² Karagas, M. R.; Choi, A. L.; Oken, E.; Horvat, M.; Schoeny, R.; Kamai, E.; Cowell, W.; Grandjean, P.; Korrick, S. Evidence on the Human Health Effects of Low-Level Methylmercury Exposure. *Environ. Health. Perspect.* **2012**, 120(6), 799-806 ; DOI:10.1289/ehp.1104494.
- ²¹³ Brambilla, G.; Abete, M. C.; Binato, G.; Chiaravalle, E.; Cossu, M.; Dellatte, E.; Miniero, R.; Orletti, R.; Piras, P.; Roncarati, A.; Ubaldi, A.; Chessa, G. Mercury occurrence in Italian seafood from the Mediterranean Sea and possible intake scenarios of the Italian coastal population. *Regul. Toxicol. Pharmacol.* **2013**, 65, 269-277 ; DOI 10.1016/j.yrtph.2012.12.009.
- ²¹⁴ Amos, H. M.; Jacob, D. J.; Streets, D. G.; Sunderland, E. M. Legacy impacts of all-time anthropogenic emissions on the global mercury cycle. *Global Biogeochem. Cy.* **2013**, 27, 410–421 ; DOI 10.1002/gbc.20040.
- ²¹⁵ Amos, H. M.; Jacob, D. J.; Kocman, D.; Horowitz, H. M.; Zhang, Y.; Dutkiewicz, S.; Horvat, M.; Corbitt, E. S.; Krabbenhoft, D. P.; Sunderland, E. M. Global biogeochemical implications of mercury discharges from rivers and sediment burial. *Environ. Sci. Technol.* **2014**, 48, 9514–9522 ; DOI 10.1021/es502134t.
- ²¹⁶ Amos, H. M.; Sonke, J. E.; Obrist, D.; Robins, N.; Hagan, N.; Horowitz, H. M.; Mason, R. P.; Witt, M.; Hedgecock, I. M.; Corbitt, E. S.; Sunderland, E. M. Observational and modeling constraints on global anthropogenic enrichment of mercury. *Environ. Sci. Technol.* **2015**, 49, 4036–4047. Doi.org/10.1021/es5058665.
- ²¹⁷ Schartup, A. T.; Balcom, P. H.; Soerensen, A. L.; Gosnell, K. J.; Calder, R. S. D.; Mason, R. P.; Sunderland, E. M. Freshwater discharges drive high levels of methylmercury in Arctic marine biota. *Proc. Natl. Acad. Sci.* **2015**, 112, 11789–11794 ; DOI 10.1073/pnas.1505541112.
- ²¹⁸ Soerensen, A. L.; Jacob, D. J.; Schartup, A. T.; Fisher, J. A.; Lehnerr, I.; St. Louis, V. L.; Heimbürger, L.-E.; Sonke, J. E.; Krabbenhoft, D. P.; Sunderland E. M. A mass budget for mercury and methylmercury in the Arctic Ocean. *Global Biogeochem. Cy.* **2016**, 30, 560–575 ; DOI 10.1002/2015GB005280.
- ²¹⁹ Soerensen, A. L.; Schartup, A. T.; Gustafsson, E.; Gustafsson, B. G.; Undeman, E.; Björn, E. Eutrophication Increases Phytoplankton Methylmercury Concentrations in a Coastal Sea—A Baltic Sea Case Study. *Environ. Sci. Technol.* **2016**, 50, 11787–11796 ; DOI 10.1021/acs.est.6b02717.
- ²²⁰ Zhang, Y.; Jaeglé, L.; Thompson, L. A.; Streets, D. G. Six centuries of changing oceanic mercury, *Global Biogeochem. Cy.* **2014**, 28, 1251–1261, doi:10.1002/2014GB004939.
- ²²¹ Zhang, Y.; Jaeglé, L.; Thompson, L. Natural biogeochemical cycle of mercury in a global three-dimensional ocean tracer model. *Global Biogeochem. Cy.* **2014**, 28(5), 553–570.
- ²²² Zhang, Y.; Jacob, D. J.; Dutkiewicz, S.; Amos, H. M.; Long, M. S.; Sunderland, E. M. Biogeochemical drivers of the fate of riverine mercury discharged to the global and Arctic oceans, *Global Biogeochem. Cy.* **2015**, 29, 854–864, doi:10.1002/2015GB005124.
- ²²³ Zhang, Y.; Horowitz, H.; Wang, J.; Xie, Z.; Kuss, J.; Soerensen, A. L. A Coupled Global Atmosphere-Ocean Model for Air-Sea Exchange of Mercury: Insights into Wet Deposition and Atmospheric Redox Chemistry. *Environ. Sci. Technol.* **2019**, 53, 5052-5061 ; DOI 10.1021/acs.est.8b06205.
- ²²⁴ Canu, D.; Rosati, G. Long-term scenarios of mercury budgeting and exports for a Mediterranean hot spot (Marano-Grado Lagoon, Adriatic Sea). *Estuar. Coast. Shelf Sci.* **2017**, 198, 518–528. DOI 10.1016/j.ecss.2016.12.005.
- ²²⁵ Sunderland, E. M.; Dalziel, J.; Heyes, A.; Branfireun, B. A.; Krabbenhoft, D. P.; Gobas, F. A. P. C. Response of a macrotidal estuary to changes in anthropogenic mercury loading between 1850 and 2000. *Environ. Sci. Technol.* **2010**, 44, 1698–1704 ; DOI 10.1021/es9032524.

-
- ²²⁶ Chen, L.; Zhang, W.; Zhang, Y.; Tong, Y.; Liu, M.; Wang, H.; Xie, H.; Wang, X. Historical and future trends in global source-receptor relationships of mercury. *Sci. Total Environ.* **2018**, *610–611*, 24–31 ; DOI 10.1016/j.scitotenv.2017.07.182.
- ²²⁷ Sunderland, E. M.; Selin, N. E. Future trends in environmental mercury concentrations: Implications for prevention strategies. *Environ. Health* **2013**, *12*, 2 ; DOI 10.1186/1476-069X-12-2.
- ²²⁸ Pakhomova, S.; Yakushev, E.; Protsenko, E.; Rigaud, S.; Cossa, D.; Knoery, J.; Couture, R.-M.; Radakovitch, O.; Yabubov, S.; Krzeminska, D.; Newton, A. Modeling the Influence of Eutrophication and Redox Conditions on Mercury Cycling at the Sediment-Water Interface in the Berre Lagoon. *Front. Mar. Sci.* **2018**, *5*, 1-15. DOI 10.3389/fmars.2018.00291.
- ²²⁹ Rajar, R.; Žagar, D.; Širca, A.; Horvat, M. Three-dimensional modelling of mercury cycling in the Gulf of Trieste. *Sci. Total Environ.* **2000**, *260*, 109–123 ; DOI 10.1016/S0048-9697(00)00555-6.
- ²³⁰ Ramsak, V.; Malacic, V.; Matjaž, L.; Kotnik, J.; Horvat, M.; Zagar, D. High-resolution pollutant dispersion modelling in contaminated coastal sites. *Environ. Res.* **2013**, *125*, 103–112 ; DOI 10.1016/j.envres.2012.12.013.
- ²³¹ Denaro, G.; Salvagio Manta, D.; Borri, A.; Bonsignore, M.; Valenti, D.; Quinci, E.; Cucco, A.; Spagnolo, B.; Sprovieri, M.; and De Gaetano, A.: HR3DHG version 1: modeling the spatiotemporal dynamics of mercury in the Augusta Bay (southern Italy). *Geosci. Model Dev.* **2020**, *13*, 2073–2093 ; DOI 10.5194/gmd-13-2073-2020.
- ²³² Casas, S.; Bacher, C. Modelling trace metal (Hg and Pb) bioaccumulation in the Mediterranean mussel, *Mytilus galloprovincialis*, applied to environmental monitoring. *J. Sea Res.* **2006**, *56*, 168–181 ; DOI 10.1016/j.seares.2006.03.006.
- ²³³ Kocman, D.; Horvat, M.; Pirrone, N.; Cinnirella, S. Contribution of contaminated sites to the global mercury budget. *Environ. Res.* **2013**, *125*, 160–170 ; DOI 10.1016/j.envres.2012.12.011.
- ²³⁴ Onrubia, J. A. T.; Petrova, M. V.; Puigcorbé, V.; Black, E. E.; Valk, O.; Dufour, A.; Hamelin, B.; Buesseler, K. O.; Masqué, P.; Le Moigne, F. A. C.; Sonke, J. E.; Rutgers van der Loeff, M.; Heimbürger-Boavida, L.-E. Mercury Export Flux in the Arctic Ocean Estimated from ²³⁴Th/ ²³⁸U Disequilibria. *ACS Earth Sp. Chem.* **2020**, *4*(5), 795-801 ; DOI 10.1021/acsearthspacechem.0c00055.
- ²³⁵ Hammerschmidt, C. R.; Bowman, K. L. Vertical methylmercury distribution in the subtropical North Pacific Ocean. *Mar. Chem.* **2012**, *132–133*, 77–82 ; DOI 10.1016/j.marchem.2012.02.005.
- ²³⁶ Mason, R. P.; Choi, A. L.; Fitzgerald, W. F.; Hammerschmidt, C. R.; Lamborg, C. H.; Soerensen, A. L.; Sunderland, E. M. Mercury biogeochemical cycling in the ocean and policy implications. *Environ. Res.* **2012**, *119*, 101–117 ; DOI 10.1016/j.envres.2012.03.013.
- ²³⁷ Lehnher, I.; St Louis, V. L.; Hintelmann, H.; Kirk, J. L. Methylation of inorganic mercury in polar marine waters. *Nat. Geosci.* **2011**, *4*, 298-302 ; DOI 10.1038/NGEO1134.
- ²³⁸ Zaferani, S.; Pérez-Rodríguez, M.; Biester, H. Diatom ooze—A large marine mercury sink. *Science* **2018**, *361*, 6404, 797–800. DOI 10.1126/science.aat2735.
- ²³⁹ Lazzari, P.; Solidoro, C.; Ibello, V.; Salon, S.; Teruzzi, A.; Béranger, K.; Colella, S.; Crise, A. Seasonal and inter-annual variability of plankton chlorophyll and primary production in the Mediterranean Sea: A modelling approach. *Biogeosciences* **2012**, *9*, 217–233 ; DOI 10.5194/bg-9-217-2012.
- ²⁴⁰ Cossa, D.; Martin, J. M.; Sanjuan, J. Dimethylmercury formation in the Alboran Sea. *Mar. Poll. Bull.* **1994**, *28*, 381-384.
- ²⁴¹ Wang, K.; Munson, K. M.; Armstrong, D. A.; MacDonald, R. W.; Wang, F. Determining seawater mercury methylation and demethylation rates by the seawater incubation approach: A critique. *Mar. Chem.* **2020**, *219*, 103753 ; DOI 10.1016/j.marchem.2020.103753.
- ²⁴² Krabbernhof, D. P.; Sunderland, E. M. Global Change and Mercury. *Science* **2013**, *341*, 1457-1458 ; DOI 10.1126/science.1242838.

-
- ²⁴³ Gittings, J. A.; Raitsoos, D. E.; Krokos, G.; Hoteit, I. Impacts of warming on phytoplankton abundance and phenology in a typical tropical marine ecosystem. *Sci. Rep.* **2018**, *8*, 2240 ; DOI:10.1038/s41598-018-20560-5.
- ²⁴⁴ Polovina, J. J.; Woodworth, P.A. Declines in phytoplankton cell size in the subtropical oceans estimated from satellite remotely-sensed temperature and chlorophyll, 1998-2007. *Deep-Sea Res. II* **2012**, *77-80*, 82-88 ; DOI 10.1016/j.dsr2.2012.04.006.
- ²⁴⁵ Osman, M. B.; Das, S. B.; Trusel, L. D.; Evans, M. J.; Fischer, H.; Grieman, M. M.; Kipfstuhl, S.; McConnell, J. R.; Saltzman, E. S. Industrial-era decline in subarctic Atlantic productivity. *Nature* **2019**, *569*, 551-555 ; DOI 10.1038/s41586-019-1181-8.
- ²⁴⁶ Pagès, R.; Baklouti, M.; Barrier, N.; Richon, C.; Dutay, J. C.; Moutin, T. Changes in rivers inputs during the last decades significantly impacted the biogeochemistry of the eastern Mediterranean basin: A modelling study. *Progr. Oceanogr.* **2020**, *181*, 102242. DOI 10.1016/j.pocean.2019.102242
- ²⁴⁷ Franz, B. A.; Karaköylül, E. M.; Siegel, D. A.; Westberry, T. K. Global Ocean phytoplankton [in state of the Climate in 2017]. *Bull. American Meteorological Soc.* **2018**, *99*(8), S94-S96.
- ²⁴⁸ Gibert, J. P. Temperature directly and indirectly influences food web structure. *Sci. Rep.* **2019**, *9*, 5312. DOI 10.1038/s41598-019-41783-0.
- ²⁴⁹ Prinn, R.; Paltsev, S.; Sokolov, A.; Sarofim, M.; Reilly, J.; Jacoby, H. Scenarios with MIT integrated global systems model: significant global warming regardless of different approaches. *Clim. Change* **2011**, *104*, 515–537 ; DOI 10.1007/s10584-009-9792-y.
- ²⁵⁰ Giorgi, F.; Gao, X.-J. Regional earth system modeling: review and future directions. *Atmosph. Oceanic Sci. Let.* **2018**, *11*, 189-197 ; DOI 10.1080/16742834.2018.1452520.